1 MS No: acp-2016-1087

2 Title: Long-term change in the contributions of various source regions to surface ozone over Japan

3 Author(s): T. Nagashima et al.

4

5 **Response to the comment of Referee #1**

6 The authors greatly appreciate your critical reading of our manuscript and highly valuable suggestions and comments.

7 Our responses to your comments are listed below. (Pages and lines are those in the track-changed manuscript)

8

9 (RC): Referee Comment / (AR): Author Response

10

11 **Major comments:**

12 (RC) The paper is thoroughly written, but reads a bit too descriptive and too technically detailed. I would encourage

13 the authors to make a bit more effort in reorganizing the sentences and try to put focus on the major scientific

14 findings in this work.

15 (AR) Thank you for the overall comment. I read through the manuscript and checked the points which seems too

16 descriptive and technically detailed, and delated or modified them if I could. The list of changes in the manuscript is

17 below.

18 **-P2, L39**

19 **-P4, L138-140 / L145-147**

20 **-P5, L180 / L183-184 / L204 / 206**

21 **-P6, L250 / L256-257**

22 **-P7, L304 / L306-307**

23 **-P8, L322-323 / L326-328 / L360-361 / L364-365**

24 **-P9, L366 / L378-379 / L407**

25 **-P10, L447-449 / L457**

26 **-P11, L458 / L466-468 / L490-491**

27 **-P12, L511**

28

29 (RC) Why up to 2005? and why surface ozone? Needs a bit of more sentences to justify these points.

30 (AR1) The model simulation should include the period starting from 1980s and covering after the year 2000 to a

31 certain extent to cover the years reported to have increasing trend in the surface O_3 over Japan. Therefore, I selected

32 the REAS v1.2 inventory because it was the only inventory data at the time of model calculation covering from 1980

33 to 2005 and focused on the whole East and Southeast Asian regions. The simulation period covering up to 2005 is

34 mainly due to the temporal coverage of the emission inventory data used (REASv1.2). However, I'm strongly sure

35 that I could obtain the basic understanding about the role of various source regions on the recent reported trend in

36 surface O_3 over Japan even with the simulation up to 2005 in this study, although I know the anthropogenic emission

37 of air pollutants in Asian region has been varied continuously even after 2005 and examining its impact on the air

38 quality in Japan is also important. I added the following sentence to justify the reason more clearly **(P4, L159-162)**.

1 *"The end of simulation period (2005) was determined mainly due to the temporal coverage of the Asian emission*

2 *data described below, however, this period sufficiently covered the years reported to have increasing trend in*

3 *surface O_3 over Japan in the previous literatures."*

4

5 (AR2) The long-term increasing trend of the surface O_3 in Japan during the last about 30 years despite of the

6 continuous efforts to reduce the emission of O_3 precursors in Japan and the consequent high violation rate of national

7 ambient air quality standard (AAQS) in Japan, almost all the ambient air monitoring sites has been failed to meet the

8 AAQS for a long time, are the persistent issues for environmental administration in Japan, therefore I focused on the

9 surface O_3. I added and modified the sentences stating the reason more clearly as follows **(P2, L84 – P3, L92).**

10 *"In Japan, analysis of long-term observations by the ambient air quality monitoring network … until the present*

11 *(Ohara and Sakata, 2003; … Akimoto et al., 2015). And the consequent high violation rate of national ambient*

12 *air quality standard (AAQS) for surface O_3 (hourly mean concentration of 60 ppbv) has been the persistent issue*

13 *in environmental administration for a long time, therefore, there is an urgent need to study the reason for the*

14 *increasing trend and examine the countermeasures. One clue is that the simultaneous observations of O_3*

15 *precursors such as … inconsistent with the increasing trend of O_3 over Japan."*

16

17 **Specific comments:**

18 (RC) Title: I would prefer to "Long-term changes in the source contribution to surface ozone in Japan", just for your

19 consideration.

20 (AR) Thank you for the suggestion. I also like the simple one. I change the title as you suggested.

21

22 (RC) Introduction, L49 - : The authors started mentioning the trends in Taiwan, China, and South Korea, but

23 historically the trends over Japan were studied with ozone sondes or surface measurements prior to these areas.

24 Hence, I would suggest the authors to start with Japanese trends then followed by recent reports in other countries.

25 (AR) Thank you for the suggestion. I changed the manuscript accordingly as follows. **(P2, L56-83)**

26 *"Japan experienced a rapid industrialization ahead of other Asian countries, and an increasing trend has been*

27 *found in various observations of tropospheric O_3 … until the mid-2000s (Tanimoto, 2009; Tanimoto et al., 2009;*

28 *Parrish et al., 2012). During the recent decades, an increasing trend in tropospheric O_3 has also been observed at*

29 *… in tropospheric O_3 for other regions in the world (Cooper et al., 2014).*

30

31 (RC) P8, L318, section 3.3: The authors phrased "IAVs" in several places in the paper. The authors use the term "IAVs"

32 not to mention (single) year-to-(single) year variability but rather decadal changes or changes during several years

33 and the next several years (Explanation of Figure 3, for example). In Figure 3 the observed IAVs are not necessarily

34 correlated with the modeled IAVs, on (single) year-by-year basis. So, I would encourage the authors to come back

35 to this point and rephrase where necessary.

36 (AR) I carefully checked all the "IAVs" and rephrased some of them which do not mean year-by-year variation but

37 rather longer (e.g. decadal) temporal variation to "long-term variation" or "temporal variation". The following is the

38 list of changes.

-P8, L334: "IVAs -> long-term variation"

-P11, L494 (title of the section 3.3): "IVAs -> temporal variations"

-P12, L513: "increase or the IAV -> temporal variation"

-P12, L514: "IVA -> temporal variation"

-P12, L542: "IVAs -> temporal variations"

-P13, L572: "IVA -> temporal variation"

-P14, L627 / L631: "IVA -> temporal variation"

-Table 2: "IAV -> Var", "InterAnnual Variation (IAV) -> Temporal Variation (Var)" <in the caption>

(RC) P7, L315-317; 2.70 and 2.58 ppbv/decade are too precise. I would suggest 2.7 and 2.6. But are these precise at 5% risk level?

(AR) Yes. These trend values are precise at 5 % risk level. So, I'll keep them as is.

(RC) P9, L374: last decade needs to be more specific. 2000s?

(AR) It means the period from 1996 to 2005. I added the period in the manuscript as follows. **(P9, L390)**

"The contribution of domestic production had a large IAV and was larger in the last decade (1996-2005) than previously."

Best regards,

Tatsuya Nagashima

1   MS No: acp-2016-1087

2   Title: Long-term change in the contributions of various source regions to surface ozone over Japan

3   Author(s): T. Nagashima et al.

4

5   **Response to the comment of Referee #2**

6   The authors greatly appreciate your critical reading of our manuscript and highly valuable suggestions and comments.

7   Our responses to your comments are listed below. (Pages and lines are those in the track-changed manuscript)

8   (RC): Referee Comment / (AR): Author Response

9

10 **General comment 1:**

11 **(RC)** This study used the NCEP renalysis data to drive the Chaser model. Please compared the meteorological

12 parameters with observations (surface or satellite) if possible. For example, cloud information and temperature.

13 This is important to ozone simulation.

14 (AR) Thank you for the comment. Unfortunately, I didn't output any cloud parameters simulated in the model, but I

15 could compare the surface temperature used in the model with those observed in Japan which were compiled by

16 Japan Meteorological Agency (JMA). JMA selected 15 sites which undergo little urban influences to derive the

17 average surface temperature over Japan. The modelled annual mean surface temperature averaged over whole Japan

18 showed a significant warming during the simulation period, 0.44 ± 0.21 °C/decade, which well matched the observed

19 warming of 0.45 ± 0.23 °C/decade. Add to this long-term trend, the inter-annual (year-to-year) variation was also

20 well captured by the model, although there was a discrepancy that the modelled temperature was somewhat warmer

21 than the observation in 2000s particularly in winter which might be related to the slight overestimation of winter

22 surface O_3 in the model depicted in the Fig.5. I added the following sentences to the manuscript. **(P12, L520-526)**

23 *"The surface temperature over Japan in the model which was assimilated into NCEP/NCAR reanalysis data*

24 *showed a warming of 0.44 ± 0.21 °C/decade in the annual mean during the simulation period which well*

25 *corresponded to the observed warming of 0.45 ± 0.23 °C/decade (JMA, 2017). The IAV of the surface temperature*

26 *was well captured by the model too, although the modelled temperature was somewhat warmer than the*

27 *observation in 2000s particularly in winter which might be related to the slight overestimation of winter surface*

28 *O_3 in the model depicted in Fig.5."*

29

30 **General comment 2:**

31 **(RC)** The author concluded that CHN contributed a lot to the trends of ozone in Japan. This can be expected because

32 China's emissions are large and increases in last decades. I encourage the authors to analyze the contributing ability

33 of each regions to JPN ozone. For example, how many is the contribution of China per NOx/VOCs emissions increase

34 to JPN O3 trends in unit: ppbv/Gg NOx or VOCs.

35 (AR) Thank you for the comment, the concept of the contributing ability is quite interesting. However, because the

36 sensitivity simulations to derive the contribution of emission trend in each region was done by varying all the O3

37 precursors emission simultaneously, it is not straightforward to estimate the contributing ability of a single O3

38 precursor individually. Nevertheless, I tried to estimate the contributing ability by conducting a multiple regression

analysis with NOx and VOC emissions in a source region (e.g CHN) as explanatory variables and the contribution of that region on the surface O_3 over Japan as the target variable, however, the analysis was failed because of the high correlation between NO_x and VOC emission trends in the source regions such as CHN (p-value of the regression coefficient for NO_x is 0.18) and KOR (that for VOC is 0.17). Therefore, deriving the contributing ability of different source regions should be addressed in the future study with a careful experimental design for that purpose.

Major comment:

(RC) The authors should gave a short discussion on the uncertainties of models and its impact on the conclusions. for example, the emission inventory. REAS should be different with other inventories (MEIC or EDGAR4). I wonders if the difference between inventories affected the conclusions.

(AR) I added a short discussion on the uncertainty of O_3 precursor emission inventories and possible impacts on the conclusions in the last chapter as follows. **(P14, L647-658)**

"The results summarized above depended largely on the forcings of long-term simulation, particularly the long-term variation of the emissions of O_3 precursors in Asia. Zhao et al. (2013) estimated the NO_x emission in China for the period 1995—2010 and compared it to the existing emission inventories including Hao et al. (2002), Zhan et al. (2007), and the version of REAS used in this study. They showed the log-term increasing trend in Chinese NO_x emission in REAS was consistent with that in the other inventories, but the amount of emission was somewhat smaller in REAS than in the others. Therefore, the long-term increasing trend in the contribution of Chinese emission to the surface O_3 over Japan showed in the preset study would be retained if the other emission inventories were used for the simulation but the specific values of the contributions could be affected. Further studies should address the impact these uncertainties in the different emission inventories on the trend of surface O_3 over Japan."

Best regards,
Tatsuya Nagashima

1 # Long-term change in the ~~contributions of various~~ source ~~regions~~contribution to surface ozone over Japan

3

4 **Tatsuya Nagashima[1], Kengo Sudo[2,3], Hajime Akimoto[1], Junichi Kurokawa[4], and**
5 **Toshimasa Ohara[1]**

6 [1]National Institute for Environmental Studies, Tsukuba, Japan

7 [2]Graduate School of Environmental Studies, Nagoya University, Nagoya, Japan

8 [3]Frontier Research Center for Global Change, Yokohama, Japan

9 [4]Asia Center for Air Pollution Research, Niigata, Japan

10 *Correspondence to:* T. Nagashima (nagashima.tatsuya@nies.go.jp)

11

Abstract

13 The relative contributions of various source regions to the long-term (1980–2005) increasing
14 trend in surface ozone (O_3) over Japan were estimated by a series of tracer-tagging
15 simulations using a global chemical transport model. The model well simulated the observed
16 increasing trend of surface O_3 including its seasonal variation and geographical features in
17 Japan and demonstrated the relative roles of different source regions in forming this trend.
18 Most of the simulated increasing trend of surface O_3 over Japan (~97 %) was explained as the
19 sum of trends in contributions of different regions to photochemical O_3 production. The
20 increasing trend in O_3 produced in China accounted for 36 % of the total increasing trend and
21 those in the other northeast Asian regions (the Korean Peninsula, coastal regions in East Asia,
22 and Japan) each accounted for about 12–15 %. Furthermore, the contributions of O_3 created in
23 the entire free troposphere and in West, South, and Southeast Asian regions also increased;
24 and their increasing trends accounted for 16 and 7 % of the total trend, respectively. The
25 impact of interannual variations in climate, in methane concentration, and in emission of O_3
26 precursors from different source regions on the relative contributions of O_3 created in each
27 region estimated above was also investigated. The variation of climate and the increase in
28 methane concentration together caused the increase of photochemical O_3 production in several
29 regions, and represented about 19 % of the total increasing trend of surface O_3 over Japan.
30 The increase in emission of O_3 precursors in China caused an increase of photochemical O_3
31 production not only in China itself but also in the other northeast Asian regions and accounted
32 for about 46 % of the total increase in surface O_3 over Japan. Similarly, the relative impact of
33 O_3 precursor emission changes in the Korean Peninsula and Japan were estimated as about 16
34 and 4 % of the total increasing trend, respectively. The O_3 precursor emission change in
35 regions other than northeast Asia caused increases in surface O_3 over Japan mainly through
36 increasing photochemical O_3 production in West, South, and Southeast Asia and the free
37 troposphere, and accounted for about 16 % of the total.

1 Introduction

Tropospheric ozone (O₃) ~~plays multiple roles in the atmosphere. O₃ itself~~ is an oxidant and photodissociates to generate the hydroxyl radical which strongly oxidizes many atmospheric compounds including various air pollutants and thus removes them from the atmosphere. In contrast, high levels of O_3 are a major air pollutant due to adverse effects on human health, natural vegetation, and agricultural produce (Wang and Mauzerall, 2004; Mauzerall et al., 2005; US EPA, 2006; Silva et al., 2013). Moreover, tropospheric O_3 is a major greenhouse gas in the atmosphere, and reduction of its amount was recently recognized as an effective measure to mitigate near-term climate change (UNEP and WMO, 2011; Shindell et al., 2012). Therefore, the spatial and temporal variations in tropospheric O_3 have been always a matter of scientific and public concern.

~~An increasing trend in tropospheric O₃ concentration has been observed during recent decades at many locations in East Asia including Taiwan (Chou et al., 2006; Chang and Lee; 2007; Li et al., 2010; Lin et al., 2010), mainland China (Lu and Wang, 2006; Ding et al., 2008; Xu et al., 2008; Wang et al., 2009; Zhang et al., 2014), and South Korea (Susaya et al., 2013; Lee et al., 2014; Seo et al., 2014). The increase rates of O₃ in those East Asian regions significantly vary depending on location and season in the range of about 0.3–3 ppbv/yr; however, the increases are generally larger than the trends in tropospheric O₃ for other regions in the world (Cooper et al., 2014).~~ Japan ~~is no exception~~experienced a rapid industrialization ahead of other Asian countries, ~~with~~ and an increasing trend has been found in various observations of O_3 over the past approximately 40 years. Routine ozonesonde measurements since 1970 at three Japanese sites of Sapporo (43° N), Tsukuba (36° N), and Kagoshima (32° N) showed an increasing trend of O_3 concentration in the lowermost troposphere up to about 1990 and relatively stable thereafter, with largest increase near the ground and discernible about 300 hPa height and below (Logan et al., 1999; Oltmans et al., 2006). With an air mass classification method based on backward air trajectories, Naja and Akimoto (2004) showed that a significant amount of the air masses reaching these ozonesonde sites in Japan spend substantial time over polluted regions in East Asia. The O_3 levels in these regionally polluted air masses increased from the 1970s to the 1990s, mainly due to large increases in nitrogen oxide ($NO_x = NO + NO_2$) emissions over China in the 1990s. Oltmans et al. (2013) analyzed a rather short period of data (1991–2010) obtained at the Ryori (39° N) surface site in north-eastern Japan and showed an increase into the mid-1990s followed by relatively little change. Other ground-based observations at a mountain site (Mt. Happo; 43° N, 1850 m asl) and three sites in the marine boundary layer along the west coast of Japan [Rishiri (45° N), Tappi (41° N), and Sado (38° N)], where few sources of pollutants exist nearby, obtained under the monitoring network of EANET (the Acid Deposition Monitoring Network in East Asia) also showed increasing trends of O_3 concentrations at least until the mid-2000s (Tanimoto, 2009; Tanimoto et al., 2009; Parrish et al., 2012). During the recent decades, an increasing trend in tropospheric O_3 has also been observed at many locations in East Asia including Taiwan (Chou et al., 2006; Chang and Lee; 2007; Li et al., 2010; Lin et al., 2010), mainland China (Lu and Wang, 2006; Ding et al., 2008; Xu et al., 2008; Wang et al., 2009; Zhang et al., 2014), and South Korea (Susaya et al., 2013; Lee et al., 2014; Seo et al., 2014). The increase rates of O_3 in those East Asian regions significantly vary depending on location and season in the range of about 0.3–3 ppbv/yr; however, the increases are generally larger than the trends in tropospheric O_3 for other regions in the world (Cooper et al., 2014).

In ~~addition~~Japan, analysis of long-term observations by the ambient air quality monitoring network mainly established in urban–suburban regions ~~in Japan~~ also showed continuous increases of surface O_3 from the mid-1980s until the present (Ohara and Sakata, 2003; Ohara

86 et al., 2008; Kurokawa et al., 2009; MOE Japan, 2013; Wakamatsu et al., 2013; Akimoto et
87 al., 2015). And the consequent high violation rate of national ambient air quality standard
88 (AAQS) for surface O_3 (hourly mean concentration of 60 ppbv) has been the persistent issue
89 in environmental administration for a long time, therefore, there is an urgent need to study the
90 reason for the increasing trend and examine the countermeasures. However, One clue is that
91 the simultaneous observations of O_3 precursors such as NO_x and non-methane hydrocarbons
92 (NMHCs) by this monitoring network revealed their decreasing trends in the same period
93 (MOE Japan, 2013), which seemed inconsistent with the increasing trend of O_3 over Japan.
94 These observed features of O_3-related atmospheric species in Japan suggest that there should
95 be an influence of transboundary transport from outside of Japan on the recent increasing
96 trend in O_3. The influence of transboundary transport on surface O_3 in East Asia was
97 examined in several studies (Sudo and Akimoto, 2007; Li et al., 2008; Nagashima et al., 2010;
98 Wang et al., 2011). Nagashima et al. (2010) demonstrated that the O_3 transported from outside
99 of Japan accounted for more than 70 % of surface O_3 over Japan in the cold season (October–
100 March) during 2000–2005, and most was attributable to O_3 from distant sources outside East
101 Asia and from the stratosphere. In the warm season (April–September), the contribution of
102 domestically created O_3 in Japan to surface O_3 over Japan increased significantly (about 20–
103 40 %), the short range intra-regional transport of O_3 from other parts of East Asia still
104 contributed about 25 %, and long range inter-regional transport of O_3 from outside East Asia
105 and the stratosphere particularly in spring could account for about half of surface O_3 over
106 Japan.

107   Therefore, the influence of O_3 from source regions outside and inside East Asia and the
108 stratosphere should be considered to explain the cause of the increasing trend in surface O_3
109 over Japan. The rapid increase in O_3 precursor emissions in East Asia in recent decades
110 (Ohara et al., 2007; Kurokawa et al., 2013) was demonstrated as a major cause of the
111 increasing trend of springtime O_3 over Japan by comparing regional chemical transport model
112 (CTM) simulations of recent decades with and without the East Asian O_3 precursor emission
113 increases during the period (Kurokawa et al., 2009; Tanimoto et al., 2009). However, they
114 only showed the springtime O_3 case and it was unclear whether the relationship held in other
115 seasons. Moreover, the relative contributions of individual countries or regions in East Asia
116 have not been well examined, particularly concerning increased surface O_3 over Japan.

117   Here, we investigated the cause of the continuous increase in surface O_3 over Japan reported
118 in the above literature, focusing on the relative contributions of various source regions over
119 the globe, particularly the contributions of individual regions in East Asia, with a long-term
120 simulation of a global CTM using the tagged tracer method. Using the same model and
121 method, Nagashima et al. (2010) showed such relative contributions of regions inside and
122 outside East Asia on surface O_3 over Japan as average values for the early 2000s. The current
123 study investigated the temporal evolution of the relative contributions of each region for the
124 26 years of 1980–2005.

125

2   Methods

2.1   Model description

128   In this study, we employed a chemistry climate model (CCM), CHASER (Sudo et al., 2002),
129 developed for the atmospheric chemistry research in the troposphere. The basic setting of the
130 model was almost identical to that used by Nagashima et al. (2010). However, the horizontal
131 resolution was modified from T63 (about 1.9° by 1.9° grid spacing in longitude and latitude)

132 to T42 (about 2.8° by 2.8°), because longer simulation period was necessary than in the
133 previous study, and so the cost of computation was reduced in the present study by selecting
134 lower horizontal resolution. There were 32 vertical layers with the top layer set at
135 approximately 40 km altitude. A detailed tropospheric photochemistry consisted of 113
136 chemical reactions and 27 photodissociation involving O_3, HO_x, NO_x, methane (CH_4), CO and
137 NMHCs calculated the temporal evolution in the concentrations of 53 chemical species. ~~The~~
138 ~~gas and liquid phase oxidation of sulfur dioxide (SO_2) and dimethyl sulfide to form the sulfate~~
139 ~~aerosol was also included in the model.~~ The concentrations of O_3 and some nitrogen
140 compounds (NO_x, HNO_3, and N_2O_5) above the tropopause that should affect tropospheric
141 chemistry were assimilated into the monthly mean output data of stratospheric CCM, because
142 the version of CHASER used was unable to calculate several chemical processes, such as
143 halogen-related chemical reactions, which are indispensable for realistic representation of
144 such chemical compounds in the stratosphere. ~~For the transport of chemical species, a semi-~~
145 ~~Lagrangian advective transport scheme (Lin and Rood, 1996; van Leer, 1997) and vertical~~
146 ~~convective transport associated with cumulus convection process were considered.~~ The model
147 also included dry and wet deposition of chemical species.

148 In this study, we conducted tracer-tagging simulation by using two different setups (full-
149 chemistry and tracer-transport setups) of CHASER. The full-chemistry setup calculated the
150 actual temporal change in the concentration of chemical species through the abovementioned
151 chemical and physical processes and outputted the chemical production and loss tendencies of
152 O_3 and related species. Then, the tracer-transport setup used the outputted chemical
153 tendencies to calculate the temporal change in the concentration of hypothetical O_3 tracers. In
154 the following subsection, the calculation procedure is briefly described.

155

2.2 Outline of the numerical simulations

2.2.1 Forcings for long-term simulation

158 Long-term simulation was performed for the period 1980–2005. The end of simulation
159 period (2005) was determined mainly due to the temporal coverage of the Asian emission data
160 described below, however, this period sufficiently covered the years reported to have
161 increasing trend in surface O_3 over Japan in the previous literatures. To drive the physical
162 properties of the model for this 26-year period, the temperature and horizontal wind velocities
163 in the model were assimilated into the National Center for Environmental Prediction/National
164 Center of Atmospheric Research (NCEP/NCAR) 6-hour reanalysis data (Kalnay et al., 1996)
165 of the corresponding year, and sea surface temperature and sea ice data of the Hadley Centre's
166 Sea Ice and Sea Surface Temperature (HadISST) data set (Rayner et al., 2003) were used in
167 the model.

168 The monthly mean stratospheric O_3 data of Akiyoshi et al. (2009) was used for the
169 assimilation above the tropopause for this period. These data were the output of a
170 stratospheric CCM simulation according to the hindcasting scenario for 1980–2004 (REF1
171 scenario) of the CCM validation activity (CCMVal) (Eyring et al., 2005), and included an
172 interannual variation (IAV) associated with the 11-year solar cycle and large declines after
173 1982 and 1991 due to the El Chichon and Pinatubo eruptions, respectively, in addition to a
174 continuous decreasing trend during the whole period. Although the simulated declines of
175 stratospheric O_3 due to the two large volcanic eruptions were somewhat overestimated, the
176 simulated IAVs in stratospheric O_3 reasonably well represented those observed with a total

177   ozone mapping spectrometer (TOMS) from satellites (Akiyoshi et al., 2009). Incidentally, the
178   stratospheric O_3 data of 2004 were used for 2005.

179   The long-term variation of the emissions of O_3 precursors (NO_x, CO, and NMHCs) ~~and SO₂~~
180   were taken from multiple emission inventories. For anthropogenic emissions in Asia, the
181   Regional Emission inventory in ASia (REAS ver.1.2) (Ohara et al., 2007) was used for each
182   year in the whole simulation period (1980–2005)~~; the REAS emission data were available for~~
183   ~~each year in the period~~. Kurokawa et al. (2009) used these emission data with a regional air
184   quality model representing well the interannual variability of surface O_3 over Japan for
185   similar period (1981–2005) to the present study. For anthropogenic emissions outside Asia, a
186   combination of three versions of EDGAR (Emission Database for Global Atmospheric
187   Research) emission data was used: EDGAR-HYDE (Van Aardenne et al., 2001) for 1980 and
188   1990; EDGAR v3.2 (Olivier and Berdowski, 2001) for 1990 and 1995; and EDGAR v3.2 Fast
189   Track 2000 (FT2000) (Olivier and Berdowski, 2001) for 2000. Because several emission
190   sectors considered in EDGAR v3.2 were not considered in EDGAR-HYDE, the emissions for
191   1990 in EDGAR-HYDE were generally smaller than in EDGAR v3.2. Therefore, we used
192   EDGAR v3.2 data for 1990, and also scaled them to estimate emission data for 1980 rather
193   than simply using EDGAR-HYDE data for 1980. For that, we scaled EDGAR v3.2 data for
194   1990 so that the ratio (r) of the difference between 1980 (f_1) and 1990 data (f_2) and their
195   average in EDGAR-HYDE [i.e., $r = (f_2 - f_1)/(f_1 + f_2)/2$] equaled the corresponding ratio (R)
196   calculated from 1990 data in EDGAR v3.2 (F_2) and 1980 data scaled from it (F_1) [i.e., $R = (F_2$
197    $- F_1)/(F_1 + F_2)/2$]. We calculated F_1 from the known values of f_1, f_2, and F_2 using the equation
198    $r = R$. Since EDGAR emission data were not available for each year but for every 10 or 5
199   years in the simulation period, the emissions for intermediate years were interpolated, and
200   FT2000 data used for years after 2000. The vegetation fire emission data developed in the
201   REanalysis of the TROpospheric chemical composition over the past 40 years project
202   (RETRO) (Schultz et al., 2008) were used for O_3 precursor emissions from biomass burning
203   ~~for the whole land area. RETRO data were available~~ for each year until 2000 in the simulation
204   period, and data for 2000 were used for years after 2000. Historical transition of the
205   atmospheric concentrations of carbon dioxide, nitrous oxide ~~(N₂O)~~, and CH_4 were prescribed
206   with those used in Nozawa et al. (2005), which were somewhat old estimations of the
207   historical evolution in greenhouse gas concentrations, but not much different from recent
208   estimations such as for the Representative Concentration Pathways (RCPs) (Meinshausen et
209   al., 2011). The difference in the concentrations between both estimations were generally
210   within a couple of percent in the simulation period.

211   The linear trends of NO_x and NMVOC annual emissions used in this study in the simulation
212   period of 1980–2005 are shown in Fig. 1. The long-term trends of emissions of both species
213   showed generally similar geographical features to each other; large decrease trends in central
214   Europe, Scandinavia, western Russia, and Kazakhstan, whereas there were widely spread
215   increasing emissions in West, South, Southeast, and East Asia, almost all Africa and Central
216   and South America except for inland Brazil. In North America, NO_x emission generally
217   decreased in the simulation period except for the west coast and New England area of the
218   USA, but that of NMVOC mostly increased with a few patchy exceptions. The trends of NO_x
219   and NMVOC emissions mentioned above were mainly due to the change in anthropogenic
220   emissions, while the change in biomass burning emissions led to a discernible trend in several
221   regions such as inland Brazil and the south of Sahel.

222   The long-term evolution of annual emissions of NO_x and NMVOC over several source areas
223   in the Northern Hemisphere is shown in Fig. 2. Because the emission data were the
224   combination of three different datasets outside Asia, there were somewhat discontinuous

225 changes at the joint years (1990 and 1995) in European and North American emissions. The
226 emissions of NO_x and NMVOC over Europe had peaks around 1990 and generally decreased
227 afterward. Over North America, both species showed small long-term trends: slight decreases
228 in NO_x and slight increases in NMVOC emissions. The emissions of both species over China
229 greatly increased during the whole period. The NO_x emissions were about 4.0 times larger in
230 2005 than 1980 and correspondingly NMVOC was 2.5 times larger, which made emissions of
231 both species for China equal to or even surpassing those for Europe or North America in 2005.
232 The emissions of both species over the Korean Peninsula increased approximately 2.8 times
233 during this period. However, those over Japan showed no such increase: NO_x emission
234 decreased until 1995 and thereafter remained stable, whereas NMVOC emissions went up
235 until 1995 and then slightly decreased.

2.2.2 Tracer tagging

237 We conducted a 26-year simulation using the full-chemistry setup of CHASER with all the
238 forcings mentioned above, followed by another 26-year simulation with the tracer-transport
239 setup of CHASER which calculated the concentration of hypothetical O_3 tracers, each tagged
240 with a particular region in the model domain. The procedure to tag a tracer with each region
241 in the second simulation was the same as used by Nagashima et al. (2010) and a brief
242 description follows. In the second simulation, the transport and dry deposition of each O_3
243 tracer were calculated same as in the first simulation, however the chemical development of
244 tracers was calculated using the chemical production (P) and loss frequencies (L) of the
245 extended odd oxygen family [$O_x = O_3 + O + O(^1D) + NO_2 + 2NO_3 + 3N_2O_5 + PANs + HNO_3$
246 + other nitrates] calculated and archived in the first simulation. In the first simulation, 3D
247 fields of P and L were outputted every 6 hours. Each O_3 tracer could be lost chemically
248 everywhere in the model domain at the frequency of L, but could be chemically produced
249 only inside its tagged region. In the stratosphere ~~over the tropopause defined by the lapse rate~~,
250 the concentration of O_3 tracer tagged with the stratosphere was assimilated into the same
251 stratospheric O_3 data as used in the first simulation, but the concentration of the tracers tagged
252 with the region in the troposphere were all set to zero. The calculated concentration of each
253 tagged O_3 tracer at a given location represents the contribution of O_3 produced in each source
254 region and transported to that location.

255 ~~The horizontal and vertical separation of the model domain for the tracer tagging was also~~
256 ~~the same as used by Nagashima et al. (2010).~~ The troposphere in the model domain was
257 horizontally separated into 22 regions and each horizontal region was further separated
258 vertically between the free troposphere (FT) and the planetary boundary layer (PBL). The
259 stratosphere was considered one separate source region, that is, the model domain was
260 separated into 45 source regions. The 22 regions for horizontal separation are shown in Fig. 1
261 and each region was assigned a three-letter code (e.g., AMN for North America) which is
262 used in the following sections. For the vertical separation of the source regions in the
263 troposphere, the PBL was defined as the lowest six layers in the model (surface to about 750
264 hPa), based on the observed and modeled vertical profiles of O_3 production.

265 The long-term tracer-tagging simulation allowed estimation of the long-term variations in
266 contributions of each source region to the O_3 concentration at given receptor locations. This is
267 important information to explain the cause of the reported increasing trend in surface O_3 over
268 East Asia. However, it should be noted that the tracer-tagging simulation calculates the
269 amount of O_3 in a receptor location that was produced chemically in each source region from
270 O_3 precursors emitted both from the source region and adjacent source regions. Thus, the
271 contribution of a source region estimated in tracer-tagging simulation should not be fully

272 attributed to emissions of O_3 precursors in that source region. Emission sensitivity simulation
273 is another method of estimating the portion of O_3 fully attributable to a change in O_3 precursor
274 emissions in a source region, and takes the difference of simulated O_3 between two model
275 runs with and without perturbed O_3 precursor emissions in that source region. The resulting
276 estimations of source contributions by the two methods can differ; however, the differences
277 have not yet been well quantified. Li et al. (2008) reported that the difference between the two
278 methods could be as much as 30 % in source apportionment estimation for one location and
279 time (i.e., Mt. Tai in central eastern China in June 2006). Wang et al. (2011) found somewhat
280 larger differences in the contributions of China to domestic O_3 concentration between the two
281 methods for each month of the year, but no discussions were made for O_3 over Japan.

282 Nevertheless, we employed the tracer-tagging simulation to study the cause of reported long-
283 term change in surface O_3 over Japan mainly due to its computational efficiency. Thus, the
284 results should be carefully interpreted in terms of the difference between the source regions of
285 chemical O_3 production and those of O_3 precursor emissions. The computational efficiency
286 resulting from the tracer-tagging approach and relatively coarse horizontal resolution enabled
287 us to make several sensitivity simulations with the different combination of forcings for long-
288 term simulation. In the following sections, the simulation with the full set of long-term
289 forcings described above, hereinafter referred to as "standard" simulation, is initially analyzed.
290 This is then further interpreted using the results of sensitivity simulations; the specific settings
291 of sensitivity simulations are also described.

292

293 **3   Results and discussion**

294 **3.1   Long-term evolution of surface O_3 over Japan**

295 Nagashima et al. (2010) validated how well CHASER can reproduce the observed features
296 of surface O_3 concentrations by comparing the simulated surface O_3 concentrations with
297 observations taken during 2000–2005 at several sites mainly in rural areas in the Northern
298 Hemisphere, and CHASER successfully simulated the annual variation of surface O_3 in a
299 variety of regions. In this study, the horizontal resolution of the model differed from that used
300 in Nagashima et al. (2010); however, the model well represented the observed concentrations
301 and seasonal evolutions of surface O_3 (Fig. S1 and Table S1 in the Supplement). The surface
302 O_3 over Japan has been observed at ambient air quality monitoring stations since the early
303 1970s when severe air pollution occurred in industrial or urban areas. The monitoring data
304 have been compiled by the Atmospheric Environmental Regional Observation System
305 (AEROS). The number of stations increased since the launch of the system and, for the period
306 of simulation (1980–2005), aAbout 1000 monitoring stations widely distributed throughout
307 Japan except in the southern islands could be used for validation of the model results. The
308 monitoring data of AEROS have been used to examine the long-term variation of surface O_3
309 over Japan in several studies and showed significant increasing trends (Ohara and Sakata,
310 2003; Ohara et al., 2008; Kurokawa et al., 2009; Akimoto et al., 2015). We validated the
311 simulated surface O_3 over Japan with the AEROS data in terms of the long-term variation in
312 the following.

313 For the validation, the monitoring sites selected had continuously observed the surface O_3
314 during the simulation period (1980–2005). To ensure continuity of sites, we selected
315 monitoring sites with annual mean surface O_3 available for every year in the simulation period.
316 The annual mean data at a monitoring site was calculated as the average of monthly means
317 when available for more than 9 months, the monthly mean was calculated from daily means

7

318 when available for over 19 days per month, and the daily mean was calculated from hourly
319 means when available for more than 19 hours per day. There were 339 sites, located mainly in
320 populated areas of Japan except in the northernmost island (Hokkaido) and southern islands
321 (Nansei Islands). We first calculated the annual mean surface O_3 ~~from the observed hourly~~
322 ~~data at each monitoring site as described above~~, and then the annual means of all sites were
323 averaged to calculate the observed annual mean surface O_3 over Japan. The simulated annual
324 mean surface O_3 over Japan was calculated as the average of annual means of the model grids,
325 which included the locations of monitoring sites selected for the validation. ~~Therefore, the~~
326 ~~model grids including Hokkaido or Nansei Islands were not used to calculate the simulated~~
327 ~~annual mean.~~ The temporal variations of observed and simulated annual mean surface O_3
328 anomalies during 1980–2005 averaged over Japan are shown in Fig. 3. During the period, the
329 observed annual mean surface O_3 over Japan showed a clear increasing trend with a linear
330 increase of about 2.70 ppbv/decade, which was significant at the 5 % risk level. The simulated
331 annual mean surface O_3 over Japan also showed a significant increasing trend with a rate of
332 about 2.58 ppbv/decade, which corresponded well to the observed increase in surface O_3 over
333 Japan. The value of the linear increasing trend and the observed features of ~~IAVs~~ long-term
334 variation in surface O_3 over Japan – such as a rapid increase from the mid-1980s to the mid-
335 1990s followed by a stagnation of increase for about 7–8 years and a further increase in the
336 past several years – were reasonably well captured by the model.

337   The model also well represented the longitudinal differences in the long-term trend of
338 surface O_3 in Japan. Figure 4 shows the maps of linear trends of annual mean surface O_3
339 during 1980–2005 calculated from the model simulations and observations at AEROS
340 monitoring sites as selected for Fig. 3. The simulated annual mean surface O_3 showed an
341 increasing trend in the whole area including all of Japan and the Korean Peninsula (Fig. 4a).
342 The simulated increasing trend of annual mean surface O_3 well exceeded 2.0 ppbv/decade in
343 wide areas of Japan except for Hokkaido, and tended to be greater toward western Japan,
344 which is nearer to the Asian continent. However, the increasing trends of observed annual
345 mean surface O_3 at each monitoring site (Fig. 4b) differed greatly from each other even in
346 nearby sites, and there was no apparent longitudinal tendency in trends at individual
347 monitoring sites. However, we averaged the observed annual mean surface O_3 at individual
348 monitoring sites at longitudinal intervals (approximately 2.8°) of the model grids as shown by
349 gray rectangles (Fig. 4b) and calculated the long-term trend of averaged monitoring data at
350 each longitudinal band. The calculated increasing trends were clearly larger toward the west,
351 which was consistent with westward rise of the increasing trends of simulated data.

352   There were seasonal differences in the long-term increasing trend of surface O_3 over Japan.
353 The temporal variations of observed and simulated seasonal mean surface O_3 anomalies
354 during 1980–2005 averaged over Japan are shown in Fig. 5. The increasing trend of surface
355 O_3 over Japan in the monitoring data was greatest in spring (March–May: 4.04 ppbv/year) and
356 was also large in summer (June–August: 3.07 ppbv/year); in contrast, increasing trends were
357 relatively small in fall (September–November: 2.29 ppbv/year) and winter (December–
358 February: 1.28 ppbv/year). Seasonal dependency in the increasing trends of observed surface
359 O_3 over Japan has been previously reported (Ohara and Sakata, 2003; ~~Naja and Akimoto,~~
360 ~~2004;~~ Parrish et al., 2012). Ohara and Sakata (2003) examined almost the same O_3 monitoring
361 data in Japan as used in the present study for the period 1985–1999 and showed year-round
362 increase in surface O_3 from 1985–1987 to 1997–1999 with a greater increase in the warm
363 season (March–August) than in the rest of the year. ~~Naja and Akimoto (2004) also reported a~~
364 ~~larger increase of O_3 in the warm season between the period 1970–1985 and 1986–2002 in the~~
365 ~~boundary layer over Japan by analyzing ozonesonde data at four sites.~~ Parrish et al. (2012)

366 summarized long-term changes in lower tropospheric baseline O_3 over the world including
367 two regions in Japan (Mt. Happo and several sites in the marine boundary layer grouped as
368 one region), and showed that the increasing trend of surface O_3 was greatest in spring and
369 least in fall in these two regions. In the present study, the simulated increasing trend in
370 seasonal mean surface O_3 was also larger in the warm (spring–summer) than in the cold
371 season (fall–winter), consistent with the observed increasing trends.

372 As described above, our model captured well the basic features of long-term trends in
373 observed surface O_3 over Japan, which allowed us to use the simulated data for further
374 analysis on the source of the long-term trend in the next section.

375

3.2 Contributions of O_3 production regions

377 The tracer-tagging simulation for 1980–2005 was conducted ~~to examine the long-term~~
378 ~~variations of O_3 tracers tagged by regions of photochemical production.~~, and the IAVs in the
379 annual mean concentrations of each tagged O_3 tracer averaged over Japan are shown in Fig. 6.
380 The tagged tracers other than FT and stratosphere in Fig. 6 and the following figures represent
381 the contribution of O_3 produced in the PBL of different source regions shown in Fig. 1, where
382 contributions of several source regions were grouped into some combined source regions. It
383 should be noted that the model grids used for averaging in these figures differed from those in
384 Figs. 3–5. They encompassed almost all of Japan excluding the Nansei Islands in order to
385 examine temporal behavior of tagged O_3 tracers in all of Japan (see Fig. 4 for actual areas for
386 averaging).

387 Domestically created O_3 was the largest contribution to surface O_3 concentration averaged
388 over Japan during the whole simulation period. The contribution of domestic production had a
389 large IAV and was larger in the last decade (1996−2005) than previously.

390 The second largest contribution was the O_3 created in the FT as a whole during almost the
391 entire period. For the FT, the northern mid-latitude regions such as North Pacific (NPC),
392 Europe (EUR), North Atlantic (NAT), North America (AMN), and China (CHN) made
393 leading contributions during the period; however, the increasing trend of these contributions
394 was considerable particularly for CHN and NPC (Fig. S2). Despite such differences among
395 the regional contributions in the FT, we hereafter only considered the total of each regional
396 contribution in the FT, since it was difficult to associate a regional contribution with a
397 particular source region of O_3 precursor emissions. The precursors eventually resulted in O_3
398 production in a region in the FT can be transported longer distance due to faster wind speed in
399 the FT and therefore would be influenced by emissions from a wider range of source regions
400 than in the PBL. The total FT contribution showed an increasing trend during the period.

401 The NO_x emission from lightning was an indispensable source of NO_x in the FT. The global
402 annual lightning-NO_x emission in the current simulation was about 3.1 TgN/year averaged
403 over the entire period and showed a small but significant increase of about 0.012 TgN/year
404 (0.39 %/year). The increase in lightning-NO_x emission was a consequence of changes in
405 convection activities due to the change in climate forced into the model during the period
406 ~~(NCEP/NCAR meteorology and HadISST data)~~. However, this increase in lightning-NO_x
407 emission was not the main cause of the increase in the contribution of the total FT – because a
408 sensitivity simulation with all emissions, CH_4 concentration, and stratospheric O_3 fixed at the
409 year 1980 level but with the same temporal evolution in climate showed a quite similar
410 increase in lightning-NO_x emission but no significant increasing trend in the total FT

411 contribution. Therefore, the main cause of the increasing trend in the total FT contribution
412 was likely to be factors other than the increase in lightning-NO_x emission.

413 The contribution of stratospheric O_3 was also large during the entire period, with
414 considerable temporal fluctuations. The large decreases of stratospheric contribution in the
415 early 1980s and 1990s stemmed from the decline of stratospheric O_3 concentration due to the
416 impact of large volcanic eruptions of Mt. El Chichon in 1982 and Mt. Pinatubo in 1991,
417 respectively (Akiyoshi et al., 2009).

418 In the early 1980s, the combined contributions of far remote regions from Japan in the
419 northern mid-latitude (Remote: EUR, NAT, and AMN) made a significant contribution, the
420 fourth largest, to the surface O_3 over Japan and remained at a steady level of contribution
421 during the study period. At the same time, the contribution of CHN significantly increased
422 from the mid-1980s, overtook the contribution of Remote in the early 1990s, and became the
423 largest single regional contribution – excluding the domestic one (i.e., JPN). Moreover, the
424 contributions of O_3 produced in the Korean Peninsula (KOR), the coastal regions in East Asia
425 [E-Asia-Seas: NPC, East China Sea (ECS), and Japan Sea (JPS)], and West-South-SouthEast
426 (WSSE) Asian regions [including Middle East (MES), India (IND), Indochina and Philippines
427 (IDC), and Indonesia etc. (IDN)] also showed obvious increasing trends.

428 The linear trend (ppbv/decade) of annual mean tagged O_3 tracers during the simulation
429 period as well as that of the total O_3, which is the sum of all tagged O_3 tracers averaged over
430 whole Japan (JPN-ALL) and those averaged over three sub-regions in Japan: western (JPN-
431 W), eastern (JPN-E), and northern (JPN-N) Japan is shown in Fig. 7 (see Fig. 4 for the
432 definition of sub-regions). The trend was calculated from the annual mean concentrations.
433 The increasing trend of total O_3 averaged over JPN-ALL was 2.37 ppbv/decade, which was
434 somewhat smaller than estimated in Fig. 3 (2.58 ppbv/decade) due to inclusion of model grids
435 in JPN-N for averaging where the simulated increasing trend of O_3 was relatively small. The
436 increasing trend of total O_3 tended to be greater westward. The absolute contribution of
437 domestically produced O_3 in Japan differed among the regions – it tended to be larger in JPN-
438 E than other parts of Japan (Nagashima et al., 2010); however, there were no such regional
439 differences in long-term trends. The westward tendency of larger increasing trends in total O_3
440 over Japan was mainly due to the similar tendency in the trends of the contribution of CHN,
441 KOR, and E-Asia-Seas, which strongly suggested a large impact of intra-regional
442 transboundary air pollution in East Asia. In particular, the increasing trend in the CHN
443 contribution was the largest for all sub-regions in Japan. The increasing trend in the
444 contributions of total FT and WSSE Asia was slightly smaller for JPN-N than for other parts
445 of Japan, which also contributed to the regional differences of the trend in total O_3 over Japan.
446 ~~Interestingly, the contribution of Remote showed a small but significant increase only in JPN-~~
447 ~~N although emissions of O_3 precursors, NO_x in particular, in Remote did not increase during~~
448 ~~the period.~~ Due to the large interannual fluctuation, the linear long-term trend of the
449 stratospheric contribution was non-significant for all regions in Japan.

450 The linear trend of tagged O_3 tracers and total O_3 averaged over all of Japan in spring,
451 summer, fall, and winter is shown in Fig. 8. The increasing trends of total O_3 in decreasing
452 order were spring, summer, winter, and fall. This is quite consistent with the seasonal
453 differences in the increasing trend of O_3 observed at several Japanese sites from the 1990s to
454 2011 (Parrish et al., 2012). The increasing trend in the CHN contribution was the largest of all
455 contributions in all four seasons and the trend was particularly large in spring. The KOR
456 contribution was also larger in spring than in other seasons~~, with the trend in summer of low~~
457 ~~statistical significance due to relatively large IAVs~~. The contribution of E-Asia-Seas increased

significantly in all seasons. Seasonal differences in the increasing trend in the E-Asia-Seas contribution were small, but were slightly larger in the warm (spring–summer) than the cold season (fall–winter). The increasing trend in domestic (JPN) contribution was larger in spring than in summer similarly to the cases of CHN and KOR contributions, but trends in both seasons were non-significant; whereas those in the cold season were significantly larger than in the warm season. The FT and WSSE Asian contributions showed semi-annual change in their increasing trends; larger in summer and winter than in spring and fall. The contribution of Remote showed a significant increasing trend only in winter~~, conversely that of Central North (CN) Asian regions [Central Asia (CAS) and East Siberia (ESB)] showed small but significant decreasing trends in the cold season but non-significant trends in the warm season~~. The seasonal features in each regional contribution described above enabled explanation of the cause of the seasonality of increasing trend in total O_3 over Japan as follows. The largest increasing trend of total O_3 in spring was predominantly attributed to the large increasing trend in contributions of source regions in northeast Asia (CHN, KOR, E-Asia-Seas, and JPN). The increasing trends in the contributions of CHN, KOR, and JPN were smaller in summer, however, partly compensated by the growth of increasing trends in the FT and WSSE Asian contributions from spring to summer. In the cold season, trends for most regions were smaller than in the warm season, except for JPN. The increasing trend in contributions of northeast Asian regions differed little between fall and winter; however, those of FT, WSSE Asia, and Remote had larger increasing trends in winter than in fall, which made the increasing trend of total O_3 in winter larger than in fall.

Table 1 summarizes the linear trends of annual mean tagged O_3 tracers and the total O_3 averaged over JPN-ALL. The vast majority (about 97 %) of the trend in total O_3 was balanced with the sum of those trends in regional contributions with statistical significance. The largest contribution was from the increase of O_3 produced in CHN (0.85 ppbv/decade), which corresponded to about 36 % of the increasing trend of total O_3. The increasing trend in the contribution of the total FT was also large (0.37 ppbv/decade), representing about 16 % of the total O_3 trend. The contributions of northeast Asian regions other than CHN also increased significantly (0.34, 0.29, and 0.27 ppbv/decade for KOR, E-Asia-Seas, and JPN, respectively) and each accounted for about 12–15 % of the total O_3 trend. About 7 % of the total O_3 trend was attributable to the increasing trend in WSSE Asian contributions (0.16 ppbv/decade). The linear trends in the contributions of remaining regions ~~[CN Asia, Remote, stratosphere, and the others (OTH)]~~ were small and non-significant, and so were not important concerning the cause of reported surface O_3 increase over Japan.

3.3 Impact of ~~IAVs~~ temporal variations in O_3 precursor emissions in different source regions on regional O_3 production

The results in the preceding section revealed the relative importance of O_3 produced in different regions to the recent increasing trend in surface O_3 over Japan. It is noteworthy that this does not indicate the relative importance of the different regions of O_3 precursor emissions. For example, there were significant contributions of E-Asia-Seas to the increasing trend in surface O_3 over Japan, but there were clearly no large emission sources of precursors in these maritime regions other than navigation. The increasing trend in the contribution of E-Asia-Seas was likely a consequence of increased transport of O_3 precursors to this region, which had been emitted in adjacent land areas. However, the tracer-tagging approach cannot distinguish the differences in origins of emissions of precursors that resulted in O_3 production in E-Asia-Seas. To further investigate the roles of different regions in the recent increasing

505 trend of surface O$_3$ over Japan, we performed a series of sensitivity simulations with different
506 assumptions for the temporal variation of factors, which would affect the surface O$_3$ over
507 Japan. Each sensitivity simulation consisted of a 26-year simulation with full-chemistry setup
508 of CHASER followed by another 26-year simulation with tracer-tagging setup of CHASER.
509 Initially, a sensitivity simulation was performed that was only forced by the IAVs in the
510 climate ~~(NCEP/NCAR meteorology and HadISST data)~~ but with all emissions of O$_3$
511 precursors, CH$_4$ concentration, and stratospheric O$_3$ fixed at the year 1980 level; then we
512 gradually added the ~~increase or the IAV~~temporal variation of chemical factors as summarized
513 in Table 2. The simulation F, driven by the ~~IAV~~ temporal variation of all forcings, was
514 identical to the standard simulation; and simulation A was mentioned concerning lightning-
515 NO$_x$ emission in the preceding section (3.2).

516 The linear trends of annual mean total O$_3$ and tagged O$_3$ tracers that had significant effects
517 on the standard simulation averaged over all of Japan in all simulations are shown and
518 compared in Fig. 9. Simulation A showed no obvious increasing trend in total O$_3$ over Japan.
519 The surface temperature over Japan in the model which was assimilated into NCEP/NCAR
520 reanalysis data showed a warming of 0.44 ± 0.21 °C/decade in the annual mean during the
521 simulation period which well corresponded to the observed warming of 0.45 ± 0.23 °C/decade
522 (JMA, 2017). The IAV of the surface temperature was well captured by the model too,
523 although the modelled temperature was somewhat warmer than the observation in 2000s
524 particularly in winter which might be related to the slight overestimation of winter surface O$_3$
525 in the model depicted in Fig.5. The JPN and total FT contributions exhibited increasing trends
526 (0.12 and 0.06 ppbv/decade, respectively), likely due to the IAV of the climate, but they were
527 non-significant.

528 The increase in atmospheric concentration of CH$_4$ was added in simulation B, because this
529 would have a non-negligible impact on tropospheric O$_3$ (background O$_3$ in particular), as
530 frequently reported (Brasseur et al., 2006; Kawase et al., 2011; HTAP, 2010 and references
531 therein). In the simulations other than A, we used a CH$_4$ concentration increase rate of about
532 12.3 ppbv/year (0.73 %/year) during 1980–2000 and flattened thereafter. In simulation B, the
533 contribution of the total FT showed a significant increasing trend (0.18 ppbv/decade) as did
534 that of Remote (0.08 ppbv/decade; data not shown). The contributions of several other regions
535 such as CHN, E-Asia-Seas, and WSSE Asia also showed slight increasing trends
536 (approximately 0.01–0.02 ppbv/decade), although non-significant. Note that these values
537 included the impact of CH$_4$ increase as well as the IAV of the climate and, consequently, the
538 total O$_3$ in simulation B showed a significant increasing trend of about 0.44 ppbv/decade,
539 representing about 19 % of the increasing trend in total O$_3$ in the standard simulation (2.37
540 ppbv/decade).

541 In simulations C–E, the ~~IAVs~~temporal variations in emission of O$_3$ precursors in northeast
542 Asian regions were gradually added: CHN, KOR, and JPN, respectively. The increase in
543 emissions of O$_3$ precursors in CHN in simulation C caused a large significant increasing trend
544 in the contribution of CHN itself (0.83 ppbv/decade). Moreover, the emission increase in
545 CHN also had a large impact on the contributions of other regions, in particular, the increase
546 trends in the contributions of KOR and E-Asia-Seas became significant: 0.12 and 0.15
547 ppbv/decade, respectively. The JPN and the total FT contributions also showed somewhat
548 larger increasing trends in simulation C than in B, but the growth in trends between the two
549 simulations was not as large as those of KOR and E-Asia-Seas. The total effect of the
550 emission increase in CHN on the increasing trend in surface O$_3$ over Japan, assessed using the
551 difference in total O$_3$ trend between simulations B and C, was about 1.08 ppbv/decade and
552 corresponded to about 46 % of the increasing trend in total O$_3$ in the standard simulation. The

relative contribution of CHN as a source region of O_3 production to the surface O_3 increasing trend over Japan was estimated as 36 % in the preceding section (3.2); however, the contribution of CHN as a source region of O_3 precursors emission was somewhat (10 %) larger due to the production of O_3 outside CHN. It is noteworthy that the slight increasing trend in the contribution of WSSE Asia shown in the CH_4 increase in simulation B was smaller in simulation C. The contributions of Remote and the stratosphere showed similar responses. The increase in O_3 precursor emissions in CHN seemed to partly offset the increase in influence of long range transport of O_3 from such regions.

The increase in emissions from KOR in addition to CHN in simulation D gave rise to a much larger increasing trend in the contributions of KOR itself (0.38 ppbv/decade). Compared with simulation C (0.12 ppbv/decade), about one-third of the increasing trend in the contribution of KOR was attributed to the O_3 precursor emission increase in CHN and the rest to emission increase in KOR. Similarly, the emission increase in KOR caused a larger increasing trend in the contributions of E-Asia-Seas in simulation D (0.25 ppbv/decade). We attributed about half of the increasing trend in the contribution of E-Asia-Seas in the standard simulation (0.29 ppbv/decade) to the impact of O_3 precursor emission increase in CHN (and partly that of the CH_4 increase: 0.15 ppbv/decade) as shown in simulation C, about one-third to that in KOR, and the rest to that in regions other than northeast Asia. By further adding the ~~IAV~~ temporal variation in the domestic (JPN) emissions in simulation E, the increasing trend in the domestic contribution became significant (0.28 ppbv/decade), implying that the increasing trend in domestically produced O_3 was from a combination of multiple factors each of which did not cause a significant increase. The total effect of the emission increase in KOR on the increasing trend in surface O_3 over Japan assessed as the difference between simulations C and D was about 0.38 ppbv/decade; and that of the IAV of domestic emission in Japan assessed as the difference between simulations D and E was about 0.09 ppbv/decade; each of which corresponded to about 16 and 4 % of the increasing trend in total O_3 in the standard simulation, respectively.

The IAV in emissions of O_3 precursors in northeast Asian regions (CHN, KOR, and JPN) together with the IAV in the climate and the increase in CH_4 concentration induced a significant increasing trend in total O_3 over Japan with a rate of 1.99 ppbv/decade. This accounted for about 84 % of the increasing trend in total O_3 in the standard simulation. The rest of the increasing trend should be regarded as from O_3 precursor emission changes in regions other than northeast Asia. The difference between simulations E and F (standard simulation) showed that the emission change in such regions influenced surface O_3 over Japan mainly through increasing the O_3 production in WSSE Asia and the FT (Fig. 9).

4   Summary and conclusion

We demonstrated the relative importance of the regions of photochemical O_3 production in the global atmosphere on the long-term increasing trend in surface O_3 over Japan reported in recent decades by conducting a series of tracer-tagging simulations using the global CTM CHASER. The impact of the IAVs of climate, of CH_4 concentration, and of emission of O_3 precursors (NO_x and NMVOC) in different source regions on regional photochemical O_3 production were also investigated.

The observed increasing trend of surface O_3 over Japan for 1980–2005 (2.70 ppbv/decade for annual mean over whole Japan) was successfully reproduced by the model (2.58 ppbv/decade) including an obvious tendency of increase toward western Japan and to be greater in the warm (spring–summer) than in the cold season (fall–winter).

The absolute contribution of each photochemical O_3 production region to the surface O_3 over Japan represented by the concentrations of tagged O_3 tracer showed different temporal evolution by regions. The contributions of all Asian regions except the northern part (i.e., CHN, KOR, E-Asia-Seas, JPN, and WSSE) as well as those of the total FT exhibited significant increasing trends during the period. The increasing trend in the contribution of domestically produced O_3 in Japan (i.e., JPN) did not differ much among the different regions in Japan. However, there was a tendency in the increasing trends in contributions of CHN, KOR, and E-Asia-Seas to be large toward western Japan, which was a main cause of the same tendency in the increasing trend in total O_3 and suggested a large impact of intra-regional transboundary air pollution in East Asia.

The trends in contributions of most O_3 production regions, except JPN, were larger in the warm than in the cold season, providing a basis for the seasonality in the increasing trend in total O_3 over Japan. Thus, the larger increasing trend of total O_3 in spring than in summer was mainly due to the same tendency in increasing trends in the contributions of northeast Asian regions (CHN, KOR, and JPN), although this was partly compensated by larger increasing trends in the FT and WSSE Asia contributions in summer than spring. In the cold season, the contributions of FT, WSSE Asia, and Remote had larger increasing trends in winter than in fall, which led to a larger increasing trend in total O_3 in winter than in fall.

The sum of the trends in contributions of O_3 production regions with sufficient statistical significance accounted for most (about 97 %) of the increasing trend in total O_3 over Japan (2.37 ppbv/decade). The largest portion was attributed to the increasing trend of O_3 produced in CHN (36 %; 0.85 ppbv/decade), followed by that in the total FT (16 %; 0.37 ppbv/decade). The increasing trend in contributions of the other northeast Asian regions (KOR, E-Asia-Seas, and JPN; 0.27–0.34 ppbv/decade) each accounted for about 12–15 % of the total O_3 trend, and the majority of the rest of the total O_3 trend (7 %; 0.16 ppbv/decade) was attributable to WSSE Asia.

We further investigated the impact of the ~~IAV~~ temporal variation of controlling factors, such as climate, CH_4 concentration, and emission of O_3 precursors, on photochemical O_3 production in different source regions and its influence on the long-term increasing trend in surface O_3 over Japan through a series of sensitivity simulations that gradually added the ~~IAV~~ temporal variation of these factors. The IAV of the climate and the increase in CH_4 concentration together caused the increase of photochemical O_3 production in several regions and resulted in the significant increasing trend in surface O_3 over Japan (0.44 ppbv/decade) and represented about 19 % of the increasing trend in surface O_3 in the standard simulation. The increase in emission of O_3 precursors in CHN led to the increase of photochemical O_3 production in northeast Asian regions including CHN itself, KOR, JPN, and E-Asia-Seas; and the resulting increasing trend in surface O_3 over Japan (1.08 ppbv/decade) accounted for about 46 % of that in the standard simulation. The relative contribution of CHN to the surface O_3 increasing trend over Japan as the source region of O_3 precursor "emission" was 10 % larger than as the source region of O_3 "production" due to production of O_3 outside of CHN. Then, the impact of the O_3 precursor emission change in KOR and JPN on the increasing trend in surface O_3 over Japan (about 0.38 and 0.10 ppbv/decade, respectively) corresponded to 16 and 4 % of the increasing trend in total O_3 in the standard simulation, respectively. The rest of the increasing trend in total O_3 in the standard simulation (about 16 %) was attributed to O_3 precursor emission change in regions other than northeast Asia, mainly through increasing the photochemical O_3 production in WSSE Asia and the total FT.

The results summarized above depended largely on the forcings of long-term simulation, particularly the long-term variation of the emissions of O_3 precursors in Asia. Zhao et al. (2013) estimated the NO_x emission in China for the period 1995−2010 and compared it to the existing emission inventories including Hao et al. (2002), Zhan et al. (2007), and the version of REAS used in this study. They showed the log-term increasing trend in Chinese NO_x emission in REAS was consistent with that in the other inventories, but the amount of emission was somewhat smaller in REAS than in the others. Therefore, the long-term increasing trend in the contribution of Chinese emission to the surface O_3 over Japan showed in the preset study would be retained if the other emission inventories were used for the simulation but the specific values of the contributions could be affected. Further studies should address the impact these uncertainties in the different emission inventories on the trend of surface O_3 over Japan.

References

667 **References**

668 Akimoto, H., Mori, Y., Sasaki, K., Nakanishi, H., Ohizumi, T., and Itano, Y.: Analysis of
669   monitoring data of ground-level ozone in Japan for longterm trend during 1990–2010:
670   Causes of temporal and spatial variation, Atmos. Environ., 102, 302–310, 2015.

671 Akiyoshi, H., Zhou, L. B., Yamashita, Y., Sakamoto, K., Yoshiki, M., Nagashima, T.,
672   Takahashi, T., Kurokawa, J., Takigawa, M., and T. Imamura, T.: A CCM simulation of the
673   breakup of the Antarctic polar vortex in the years 1980–2004 under the CCMVal scenarios,
674   J. Geophys. Res., 114, D03103, doi:10.1029/2007JD009261, 2009.

675 Brasseur, G. P., Schultz, M., Granier, C., Saunois, M., Diehl, T., Botzet, M., and Roeckner,
676   E.: Impact of climate change on the future chemical composition of the global troposphere,
677   J. Clim., 19, 3932–3951, doi:10.1175/JCLI3832.1, 2006.

678 Chang, S.-C. and Lee, C.-T.: Evaluation of the trend of air quality in Taipei, Taiwan from
679   1994 to 2003, Environ. Monit. Assess., 127, 87–96, doi:10.1007/s10661-006-9262-1, 2007.

680 Chou, C. C.-K., Liu, S. C., Lin, C.-Y., Shiu, C.-J., and Chang, K.-H.: The trend of surface
681   ozone in Taipei, Taiwan, and its causes: Implications for ozone control strategies, Atmos.
682   Environ., 40, 3898–3908, 2006.

683 Cooper, O. R., Parrish, D. D., Ziemke, J., Balashov, N. V., Cupeiro, M., Galbally, I. E., Gilge,
684   S., Horowitz, L., Jensen, N. R., Lamarque, J.-F., Naik, V., Oltmans, S. J., Schwab, J.,
685   Shindell, D. T., Thompson, A. M., Thouret, V., Wang, Y., and Zbinden, R. M.: Global
686   distribution and trends of tropospheric ozone: An observation-based review, Elementa, 2,
687   000029, doi: 10.12952/journal.elementa.000029, 2014.

688 Ding, A. J., Wang, T., Thouret, V., Cammas, J.-P., and Nédélec, P.: Tropospheric ozone
689   climatology over Beijing: analysis of aircraft data from the MOZAIC program, Atmos.
690   Chem. Phys., 8, 1–13, 2008.

691 Eyring, V., Harris, N. R P., Rex, M., Shepherd, T. G., Fahey, D. W., Amanatidis, G. T.,
692   Austin, J., Chipperfield, M. P., Dameris, M., Forster, P. M. De F., Gettelman, A., Graf, H.
693   F., Nagashima, T., Newman, P. A., Pawson, S., Prather, M. J., Pyle, J. A., Salawitch, R. J.,
694   Santer, B. D., and Waugh, D. W.: A strategy for process-oriented validation of coupled
695   chemistry-climate models. Bull. Am. Meteorol. Soc., 86, 1117–1133, 2005.

696 Hao, J. M., Tian, H. Z., and Lu, Y. Q.: Emission inventories of NO_x from commercial energy
697   consumption in China, 1995–1998, Environ. Sci. Technol., 36, 552–560,
698   doi:10.1021/Es015601k, 2002.

699 HTAP, UNECE: Hemispheric Transport of Air Pollution 2010: Part A: Ozone and Particulate
700   Matter, Air Pollution Studies No. 17, (ed. by Dentener, F., Keating, T., and Akimoto, H.),
701   ECE/EN.Air/100, 2010.

702 JMA (Japan Meteorological Agency): available online at
703   http://www.data.jma.go.jp/cpdinfo/temp/list/an_jpn.html (In Japanese), 2017.

704 Kalnay, E., Kanamitsu, M., Kistler, R., Collins, W., Deaven, D., Gandin, L., Iredell, M., Saha,
705   S., White, G., Woollen, J., Zhu, Y., Leetmaa, A., Reynolds, B., Chelliah, M., Ebisuzaki,
706   W., Higgins, W., Janowiak, J., Mo, K. C., Ropelewski, C., Wang, J., Jenne, R., and Joseph,
707   D.: The NCEP/NCAR 40-year reanalysis project, Bull. Amer. Meteor. Soc., 77, 437–470,
708   1996.

709 Kawase, H., Nagashima, T., Sudo, K., and Nozawa, T.: Future changes in tropospheric ozone
710   under Representative Concentration Pathways (RCPs), Geophys. Res. Lett., 38, L05801,
711   doi:10.1029/2010GL046402, 2011.

712 Kurokawa, J., Ohara, T., Uno, I., Hayasaki, M., and Tanimoto, H.: Influence of
713   meteorological variability on interannual variations of springtime boundary layer ozone
714   over Japan during 1981–2005, Atmos. Chem. Phys., 9, 6287–6304, 2009.

715 Kurokawa, J., Ohara, T., Morikawa, T., Hanayama, S., Janssens-Maenhout, G., Fukui, T.,
716   Kawashima, K., and Akimoto, H.: Emissions of air pollutants and greenhouse gases over
717   Asian regions during 2000–2008: Regional Emission inventory in ASia (REAS) version 2,
718   Atmos. Chem. Phys., 13, 11019–11058, 2013.

719 Lee, H.-J., Kim, S.-W., Brioude, J., Cooper, O. R., Frost, G. J., Kim, C.-H., Park, R. J.,
720   Trainer, M., and Woo J.-H.: Transport of NOx in East Asia identified by satellite and in
721   situ measurements and Lagrangian particle dispersion model simulations, J. Geophys. Res.
722   Atmos., 119, 2574–2596, doi:10.1002/2013JD021185, 2014.

723 Li, J., Wang, Z. F., Akimoto, H., Yamaji, K., Takigawa, M., Pochanart, P., Liu, Y., Tanimoto,
724   H., and Kanaya, Y.: Near-ground ozone source attributions and outflow in central eastern
725   China during MTX2006, Atmos. Chem. Phys., 8, 7335–7351, 2008.

726   Li, H. C., Chen, K. S., Huang, C. H., and Wang, H. K.: Meteorologically adjusted long-term
727   trend of ground-level ozone concentrations in Kaohsiung County, southern Taiwan, Atmos.
728   Environ., 44, 3605–3608, 2010.

729   Lin, S.-J. and Rood, R. B.: Multidimensional flux-form semi-Lagrangian transport scheme,
730   Mon. Weather Rev., 124, 2046–2070, 1996.

731   Lin, Y.-K., Lin, T.-H., and Chang, S.-C.: The changes in different ozone metrics and their
732   implications following precursor reductions over northern Taiwan from 1994 to 2007,
733   Environ. Monit. Assess., 169, 143–157, 2010.

734   Logan, J. A., Megretskaia, I. A., Miller, A. J., Tiao, G. C., Choi, D., Zhang, L., Stolarski, R.
735   S., Labow, G. J., Hollandsworth, S. M., Bodeker, G. E., Claude, H., de Muer, D., Kerr, J.
736   B., Tarasick, D. W., Oltmans, S. J., Johnson, B., Schmidlin, F., Staehelin, J., Viatte, P., and
737   Uchino, O.: Trends in the vertical distribution of ozone: A comparison of two analyses of
738   ozonesonde data, J. Geophys. Res., 104, 26373–26399, 1999.

739   Lu, W.-Z. and Wang, X.-K.: Evolving trend and self-similarity of ozone pollution in central
740   Hong Kong ambient during 1984–2002, Sci. Total Environ., 357, 160–168, 2006.

741   Mauzerall, D. L., Sultan, B., Kim, N., and Bradford, D. F.: NOx emissions from large point
742   sources: variability in ozone production, resulting health damages and economic costs,
743   Atmos. Environ., 39, 2851–2866, 2005.

744   Meinshausen, M., Smith. S. J., Calvin, K., Daniel, J. S., Kainuma, M. L. T., Lamarque, J-F.,
745   Matsumoto, K., Montzka, S. A., Raper, S. C. B., Riahi, K., Thomson, A., Velders, G. J. M.,
746   and van Vuuren, D. P. P.: The RCP greenhouse gas concentrations and their extensions
747   from 1765 to 2300, Climatic Change, 109, 213–241, 2011.

748   MOE (Ministry of Environment) Japan: FY 2013 status of air pollution, available online at:
749   http://www.env.go.jp/air/osen/jokyoh25/ (in Japanese), 2013.

750   Nagashima, T., Ohara, T., Sudo, K., and Akimoto, H.: The relative importance of various
751   source regions on East Asian surface ozone, Atmos. Chem. Phys., 10, 11305–11322, 2010.

752   Naja, M. and Akimoto, H.: Contribution of regional pollution and long-range transport to the
753   Asia-Pacific region: Analysis of long-term ozonesonde data over Japan, J. Geophys. Res.,
754   109, D21306, doi:10.1029/2004JD004687, 2004.

755 Nozawa, T., Nagashima, T., Shiogama, H., and Crooks, S. A.: Detecting natural influence on

756   surface air temperature change in the early twentieth century, Geophys. Res. Lett., 32,

757   L20719, doi:10.1029/2005GL023540, 2005.

758 Ohara, T. and Sakata, T.: Long-term variation of photochemical oxidants over Japan, J. Jpn.

759   Soc. Atmos. Environ., 38, 47–54. (in Japanese with English summary), 2003.

760 Ohara, T., Yamaji, K., Uno, I., Tanimoto, H., Sugata, S., Nagashima, T., Kurokawa, J., Horii,

761   N., and Akimoto, H.: Long-term simulations of surface ozone in East Asia during 1980–

762   2020 with CMAQ and REAS inventory, In Air Pollution Modelling and Its Application

763   XIX (NATO Science for Peace and Security Series C: Environmental Security) (ed. by

764   Borrego, C., and Miranda, A. I.). Springer, Dordrecht, The Netherlands, 136–144, 2008.

765 Ohara, T., Akimoto, H., Kurokawa, J., Horii, N., Yamaji, K., Yan, X., and Hayasaka, T.: An

766   Asian emission inventory of anthropogenic emission sources for the period 1980–2002,

767   Atmos. Chem. Phys., 7, 4410–4444, 2007.

768 Olivier, J. G. J. and Berdowski, J. J. M.: Global emissions sources and sinks, in: The Climate

769   System, Berdowski, J., Guicherit, R., and Heij, B. J. (eds.), A. A. Balkema Publishers/

770   Swets & Zeitlinger Publishers, Lisse, The Netherlands, 33–78, 2001.

771 Oltmans, S. J., Lefohn, A. S., Harris, J. M., Galbally, I., Scheel, H. E., Bodeker, G., Brunke,

772   E., Claude, H., Tarasick, D., Johnson, B. J., Simmonds, P., Shadwick, D., Anlauf, K.,

773   Hayden, K., Schmidlin, F., Fujimoto, T., Akagi, K., Meyer, C., Nichol, S., Davies, J.,

774   Redondas, A., and Cuevas, E.: Long-term changes in tropospheric ozone, Atmos. Environ.,

775   40, 3156–3173, 2006.

776 Oltmans, S. J., Lefohn, A. S., Shadwick, D., Harris, J. M., Scheel, H. E., Galbally, I., Tarasick,

777   D. W., Johnson, B. J., Brunke, E.-G., Claude, H., Zeng, G., Nichol, S., Schmidlin, F.,

778   Davies, J., Cuevas, E., Redondas, A., Naoe, H., Nakano, T., and Kawasato, T.: Recent

779   tropospheric ozone changes – A pattern dominated by slow or no growth, Atmos. Environ.,

780   67, 331–351, 2013.

781 Parrish, D. D., Law, K. S., Staehelin. J., Derwent, R., Cooper, O. R., Tanimoto, H., Volz-

782   Thomas, A., Gilge, S., Scheel, H.-E., Steinbacher, M., and Chan, E.: Long-term changes in

783   lower tropospheric baseline ozone concentrations at northern mid-latitudes, Atmos. Chem.

784   Phys., 12, 11485–11504, 2012.

785   Rayner, N. A., Parker, D. E., Horton, E. B., Folland, C. K., Alexander, L. V., Rowell, D. P.,
786   Kent, E. C., and Kaplan, A.: Global analyses of sea surface temperature, sea ice, and night
787   marine air temperature since the late nineteenth century, J. Geophys. Res., 108, 4407,
788   doi:10.1029/2002JD002670, 2003.

789   Schultz, M. G., Heil, A., Hoelzemann, J. J., Spessa, A., Thonicke, K., Goldammer, J. G., Held,
790   A. C., Pereira, J. M. C., and van het Bolscher, M.: Global wildland fire emissions from
791   1960 to 2000, Global Biogeochem. Cycles, 22, GB2002, doi:10.1029/2007GB003031,
792   2008.

793   Seo, J., Youn, D., Kim, J. Y., and Lee, H.: Extensive spatiotemporal analyses of surface
794   ozone and related meteorological variables in South Korea for the period 1999–2010,
795   Atmos. Chem. Phys., 14, 6395–6415, 2014.

796   Shindell, D., Kuylenstierna, J. C. I., Faluvegi, G., Milly, G., Emberson, L., Hicks, K., Vignati,
797   E., Van Dingenen, R., Janssens-Maenhout, G., Raes, F., Pozzoli, L., Amann, M., Klimont,
798   Z., Kupiainen, K., Höglund-Isaksson, L., Anenberg, S. C., Muller, N., Schwartz, J., Streets,
799   D., Ramanathan, V., Oanh, N. T. K., Williams, M., Demkine, V., and Fowler, D.:
800   Simultaneously mitigating near-term climate change and improving human health and food
801   security, Science, 335, 183–189, 2012.

802   Silva, R. A., West, J. J., Zhang, Y., Anenberg, S. C., Lamarque, J.-F., Shindell, D. T., Collins,
803   W. J., Dalsoren, S., Faluvegi, G., Folberth, G., Horowitz, L. W., Nagashima, T., Naik, V.,
804   Rumbold, S., Skeie, F., Sudo, K., Takemura, T., Bergmann, D., Cameron-Smith, P., Cionni,
805   I., Doherty, R. M., Eyring, V., Josse, B., MacKenzie, I. A., Plummer, D., Righi, M.,
806   Stevenson, D. S., Strode S., Szopa, S., and Zeng, G.: Global premature mortality due to
807   anthropogenic outdoor air pollution and the contribution of past climate change, Environ.
808   Res. Lett., 8, 034005, 2013.

809   Sudo, K. and Akimoto, H.: Global source attribution of tropospheric ozone: Long-range
810   transport from various source regions, J. Geophys. Res., 112, D12302,
811   doi:10.1029/2006JD007992, 2007.

812   Sudo, K., Takahashi, M., Kurokawa, J., and Akimoto, H.: CHASER: A global chemical
813   model of the troposphere: 1. Model description, J. Geophys. Res., 107(D17), 4339,
814   doi:10.1029/2001JD001113, 2002.

815   Susaya, J., Kim, K.-H., Shon, Z.-H., and Brown, R. J. C.: Demonstration of long-term
816   increases in tropospheric O_3 levels: Causes and potential impacts, Chemosphere, 92, 1520–
817   1528, 2013.

818   Tanimoto, H.: Increase in springtime tropospheric ozone at a mountainous site in Japan for
819   the period 1998–2006, Atmos. Environ., 43, 1358–1363, 2009.

820   Tanimoto, H., Ohara, T., and Uno, I.: Asian anthropogenic emissions and decadal trends in
821   springtime tropospheric ozone over Japan: 1998–2007, Geophys. Res. Lett., 36, L23802,
822   doi:10.1029/2009GL041382, 2009.

823   UNEP (United Nations Environment Programme) and WMO (World Meteorological
824   Organization): Integrated Assessment of Black Carbon and Tropospheric Ozone: Summary
825   for   Decision   Makers,   available   online   at
826   http://www.unep.org/dewa/Portals/67/pdf/Black_Carbon.pdf, 2011.

827   US EPA (U.S. Environmental Protection Agency): Air Quality Criteria for Ozone and Related
828   Photochemical Oxidants (Final), U.S. Environmental Protection Agency, Washington, DC,
829   EPA/600/R-05/004aF-cF, 2006.

830   Van Aardenne, J. A., Dentener, F. J., Olivier, J. G. J., Klein Goldewijk, C. G. M., and
831   Lelieveld, J.: A 1 x 1 degree resolution dataset of historical anthropogenic trace gas
832   emissions for the period 1890–1990, Global Biogeochem. Cy., 15(4), 909–928, 2001.

833   Van Leer, B.: Toward the ultimate conservative difference scheme. IV: A new approach to
834   numerical convection, J. Comput. Phys., 23, 276–299, 1977.

835   Wakamatsu, S., Morikawa, T., and Ito, A.: Air Pollution Trends in Japan between 1970 and
836   2012 and Impact of Urban Air Pollution Countermeasures, Asian J. Atmos. Env., 7(4),
837   177–190, 2013.

838   Wang, X. and Mauzerall, D. L.: Characterizing distributions of surface ozone and its impact
839   on grain production in China, Japan and South Korea: 1990 and 2020, Atmos. Environ., 38,
840   4383–4402, 2004.

841   Wang, T., Wei, X. L., Ding, A. J., Poon, C. N., Lam, K. S., Li, Y. S., Chan, L. Y., and Anson,
842   M.: Increasing surface ozone concentrations in the background atmosphere of Southern
843   China, 1994–2007, Atmos. Chem. Phys., 9, 6217–6227, 2009.

844 Wang, Y., Zhang, Y., Hao, J., and Luo, M.: Seasonal and spatial variability of surface ozone
845 over China: contributions from background and domestic pollution, Atmos. Chem. Phys.,
846 11, 3511–3525, 2011.

847 Xu, X., Lin, W., Wang, T., Yan, P., Tang, J., Meng, Z., and Wang, Y.: Long-term trend of
848 surface ozone at a regional background station in eastern China 1991–2006: enhanced
849 variability, Atmos. Chem. Phys., 8, 2595–2607, 2008.

850 Zhang, Q., Streets, D. G., He, K., Wang, Y., Richter, A., Burrows, J. P., Uno, I., Jang, C. J.,
851 Chen, D., Yao, Z., and Lei, Y.: NO_x emission trends for China, 1995–2004: The view from
852 the ground and the view from space, J. Geophys. Res.-Atmos., 112,
853 doi:10.1029/2007jd008684, 2007.

854 Zhang, Q., Yuan, B., Shao, M., Wang, X., Lu, S., Lu, K., Wang, M., Chen, L., Chang, C.-C.,
855 and Liu, S. C.: Variations of ground-level O_3 and its precursors in Beijing in summertime
856 between 2005 and 2011, Atmos. Chem. Phys., 14, 6089–6101, 2014.

857 Zhao, B., Wang, S. X., Liu, H., Xu, J. Y., Fu, K., Klimont, Z., Hao, J. M., He, K. B., Cofala,
858 J., and Amann M.: NO_x emissions in China: historical trends and future perspectives,
859 Atmos. Chem. Phys., 13, 9869–9897, 2013.

860
861

862   **Table 1.** Summary of the linear trends of annual mean tagged O$_3$ tracers as well as the total O$_3$

863   averaged over Japan (JPN-ALL) for 1980–2005. Bold figures denote that trends are

864   significant at 5 % risk level.

Source Region	Trend [ppbv/dec]	Percent
CHN	**0.85 ± 0.2**	35.8
KOR	**0.34 ± 0.14**	14.6
JPN	**0.27 ± 0.19**	11.5
E-Asia-Seas	**0.29 ± 0.05**	12.4
WSSE Asia	**0.16 ± 0.04**	6.8
CN Asia	-0.05 ± 0.08	-2.1
Remote	0.04 ± 0.08	1.7
OTH	0.01 ± 0.02	0.5
FT	**0.37 ± 0.1**	15.5
Strat.	0.08 ± 0.28	3.3
Total	**2.37 ± 0.42**	100.0

865

866

867 **Table 2.** Summary of the sensitivity simulations and the standard simulation

Simulation code	CH4 concentration	O3 precursor emissions				Stratospheric O3 trend
		CHN	KOR	JPN	ROW[a]	
A	1980[b]	1980	1980	1980	1980	1980
B	increase[c]	1980	1980	1980	1980	1980
C	increase	~~IAV[d]~~Var[d]	1980	1980	1980	1980
D	increase	~~IAV~~Var	~~IAV~~Var	1980	1980	1980
E	increase	~~IAV~~Var	~~IAV~~Var	~~IAV~~Var	1980	1980
F (standard)	increase	~~IAV~~Var	~~IAV~~Var	~~IAV~~Var	~~IAV~~Var	~~IAV~~Var

868 a Precursor emissions in the Rest Of the World (ROW) other than CHN, KOR, and JPN

869 b Each factor was fixed at the year 1980 level

870 c CH4 concentration increased until 2000 and flattened thereafter

871 d ~~InterAnnual~~ Temporal Variation (~~IAV~~Var) of each factor was considered

24
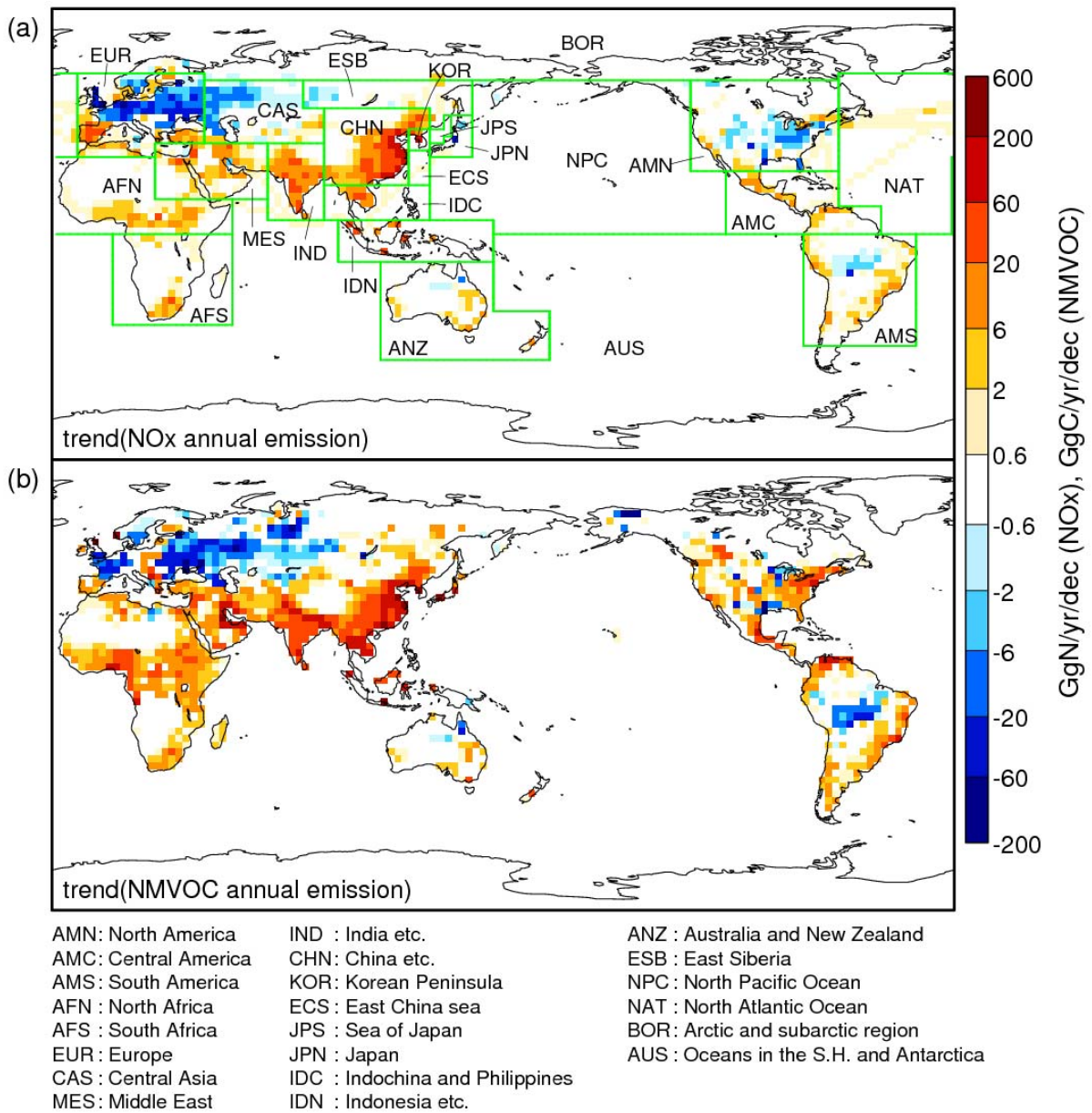
Figure 1. Linear trends of (a) NO$_x$ and (b) NMVOC emission during the simulation period (1980–2005) used in the study. Significant trends at 5 % risk level are colored. Source regions for tracer tagging are also displayed in the top figure.
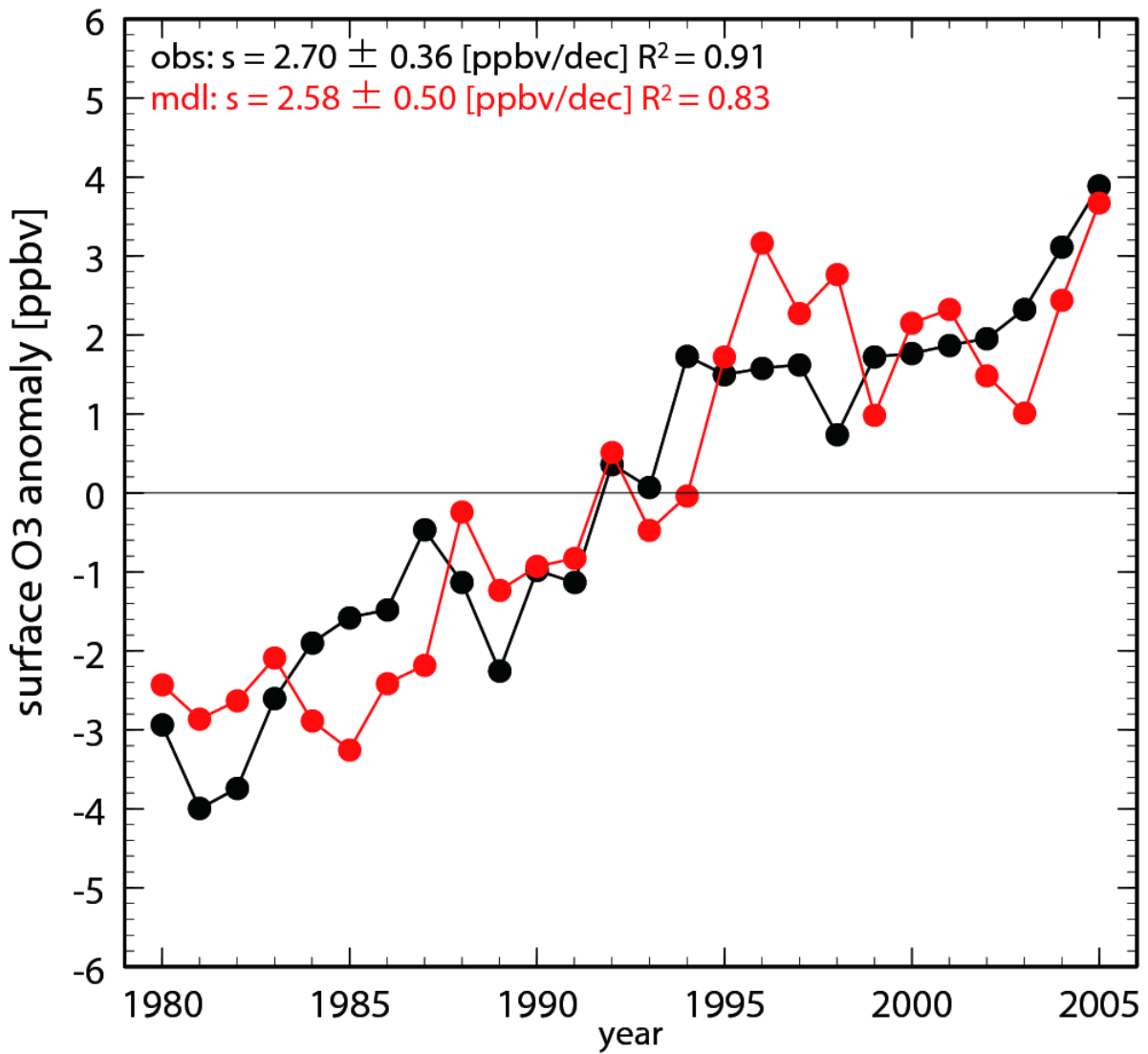
872
873
874
875

876
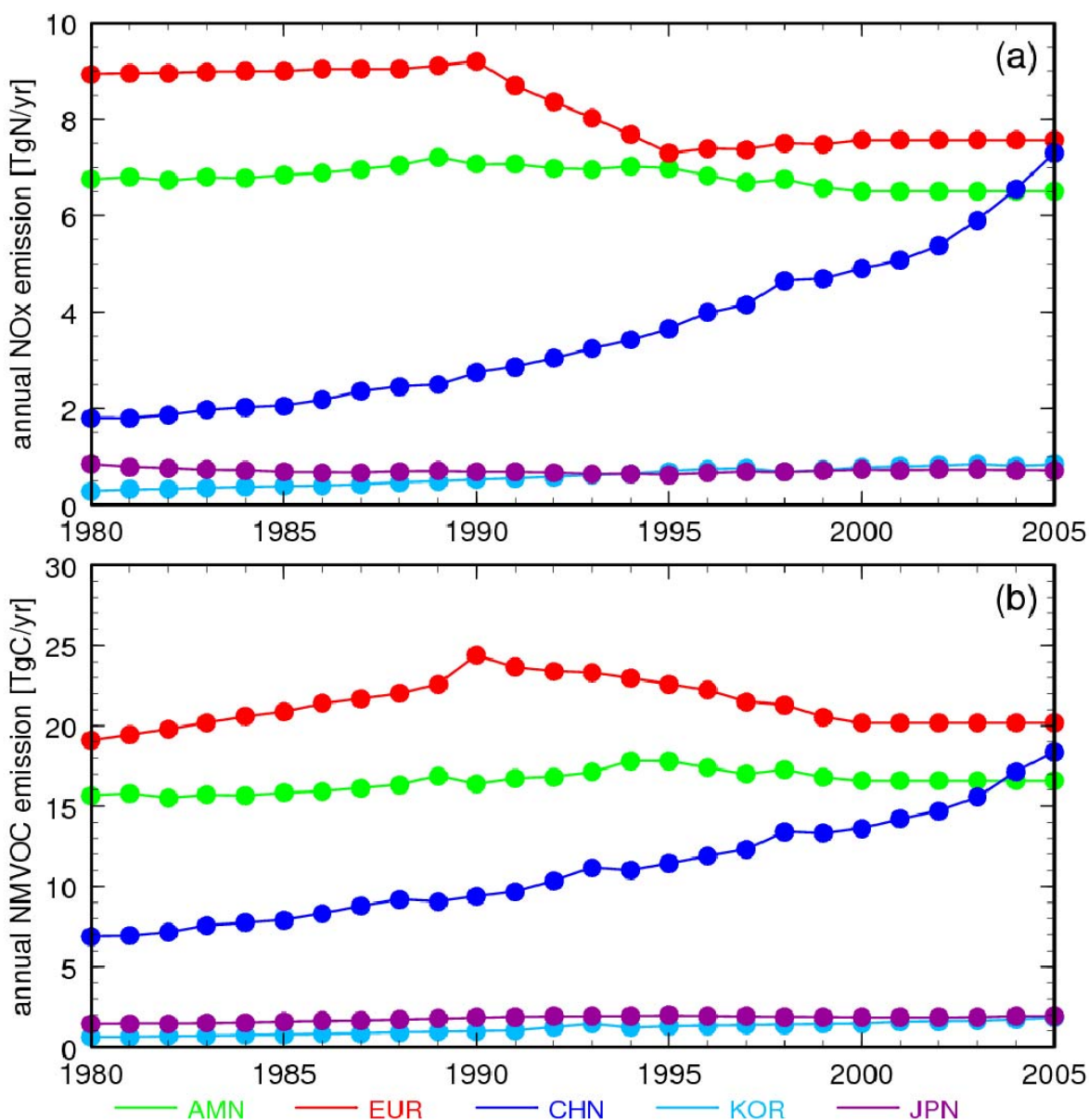
Figure 2. Temporal evolution of emissions of (a) NO$_x$ and (b) NMVOC averaged over several

source areas in the Northern Hemisphere depicted in Fig. 1.

879

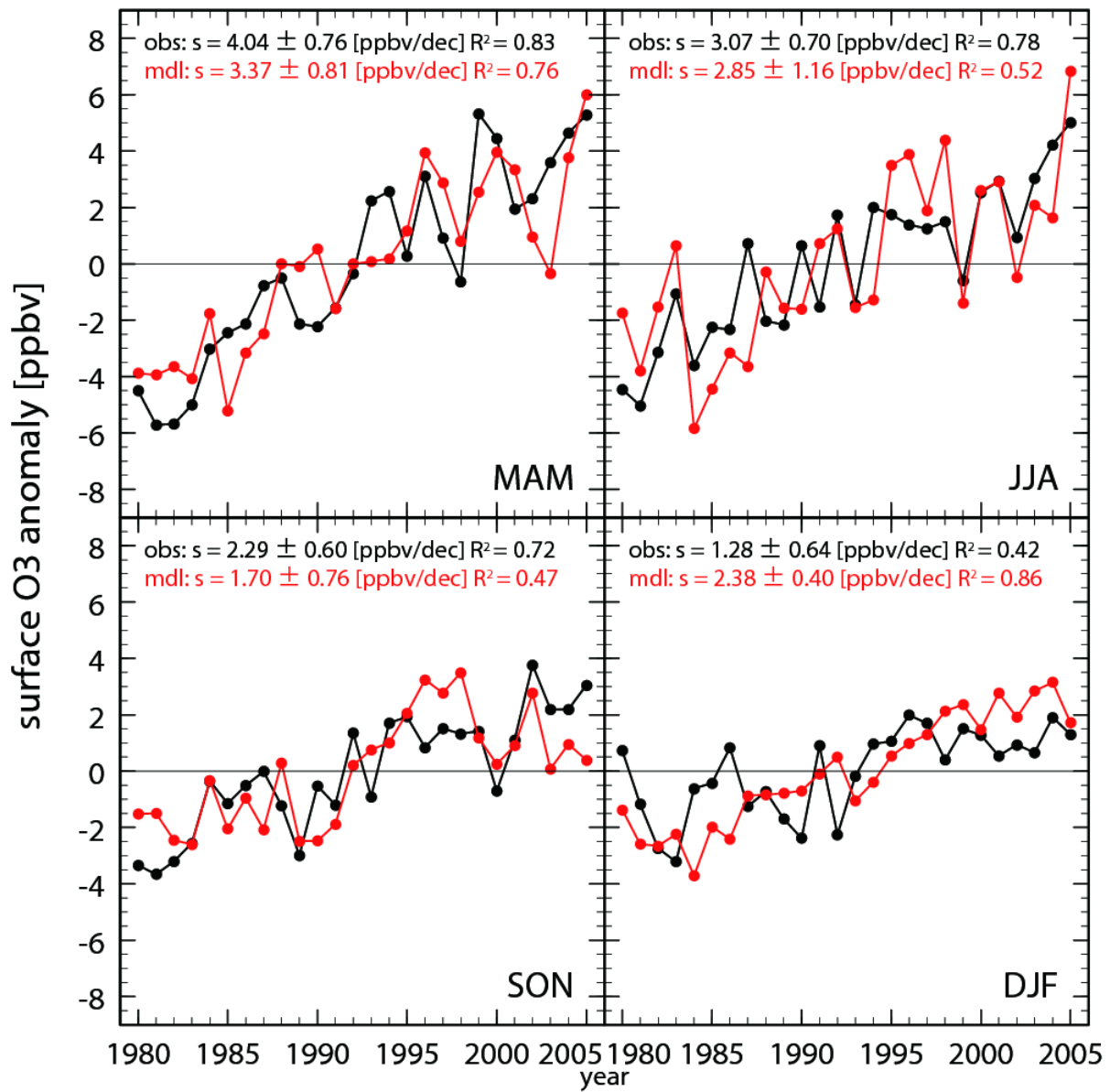880   **Figure 3.** The temporal changes of annual mean surface O_3 anomaly averaged over Japan

881   from observation (AEROS: black) and model calculation (red). Anomalies are defined as

882   deviations from the values averaged over 1980–2005. The slope of a regression (s) for 1980–

883   2005 with their 95 % confidence interval and R^2 are also shown.
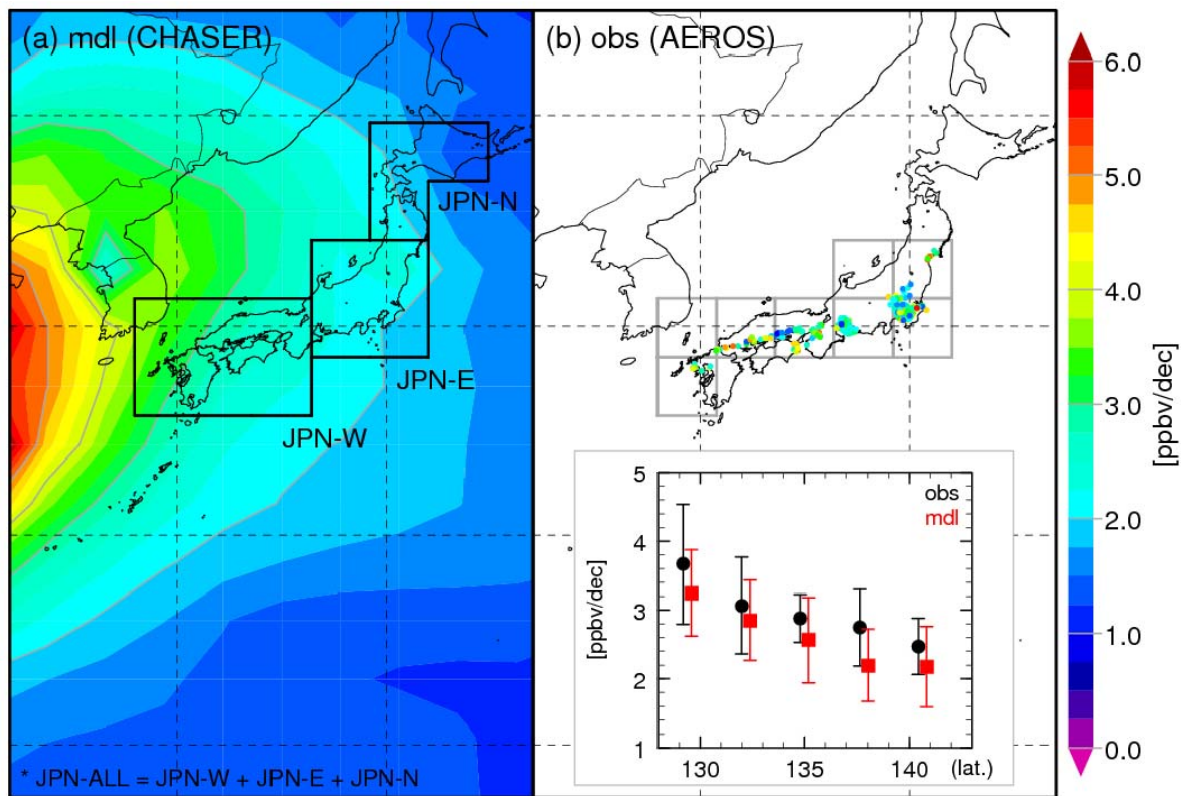
Figure 4. The linear trend of annual mean surface O_3 in 1980–2005 calculated from (a) model simulations and (b) observations at AEROS monitoring sites. The inset in figure (b) shows the longitudinal change of linear trends (black: AEROS observation; red: model) averaged within the model grids shown by gray rectangles. The error bars denote their 95 % confidence intervals. The black-rimmed areas in figure (a) are the area for averaging used in the figures from Fig. 6. Note that JPN-ALL is the sum of JPN-W, JPN-E, and JPN-N areas and used for the averaging in those figures.

892

Figure 5. Same as Fig. 3 but the temporal changes of seasonal mean surface O_3 anomaly
averaged over Japan from observations (AEROS: black) and model calculations (red).
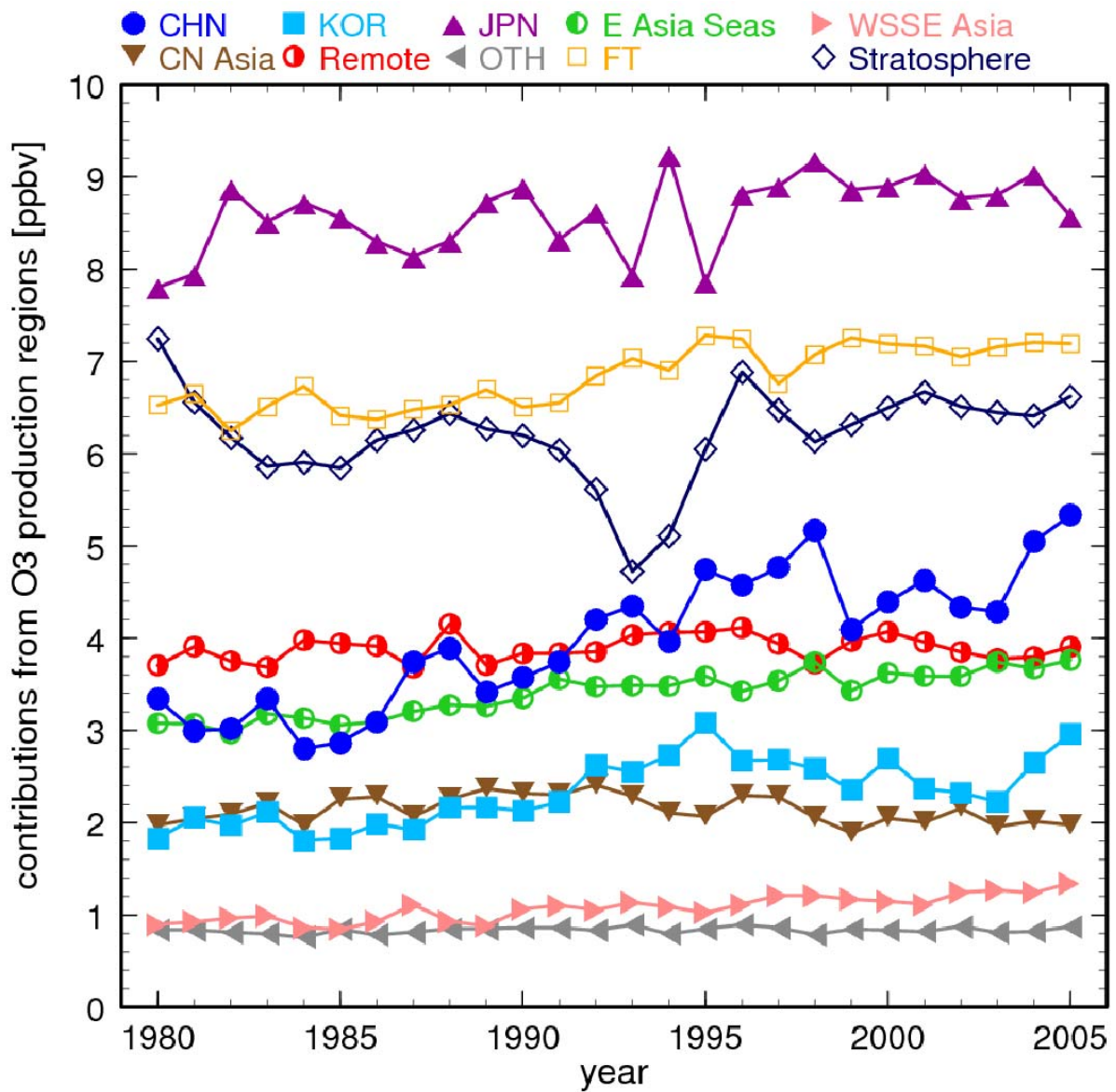
Figure 6. Long-term changes of annual mean contributions from source regions to surface O₃ over Japan. Some source regions are grouped: E-Asia-Seas is the sum of NPC, JPS, and ECS; WSSE Asia is the sum of MES, IND, IDN, and IDC; CN Asia is the sum of CAS and ESB; Remote is the sum of AMN, NAT, and EUR; and OTH is the other regions in the planetary boundary layer.
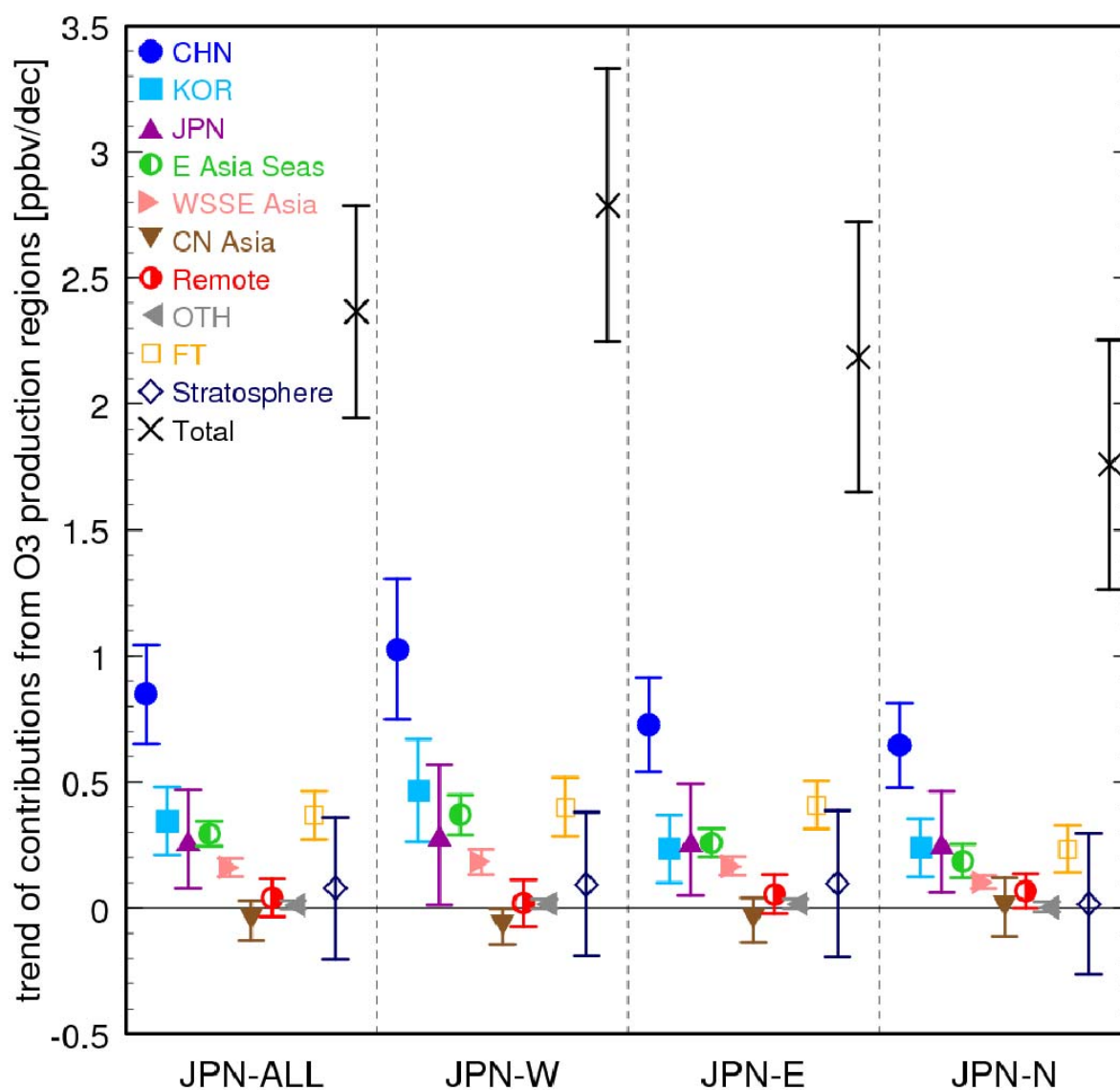
Figure 7. Linear trends of annual mean contributions in 1980–2005 from source regions to surface O_3 over Japan shown in Fig. 6 (JPN-ALL) and those averaged in three sub-regions in Japan (JPN-W, JPN-E, and JPN-N). Error bars are 95 % confidence intervals.
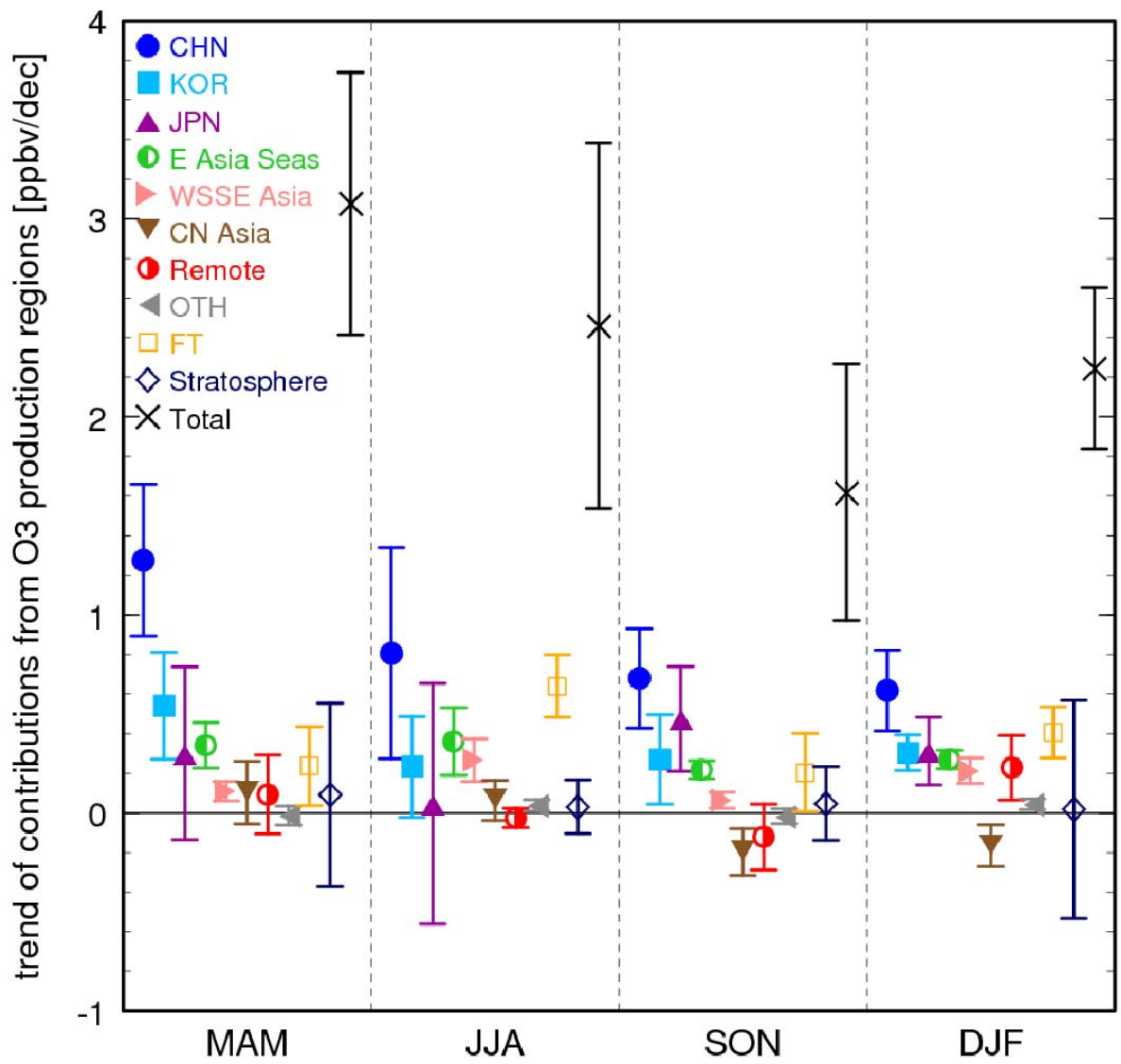
Figure 8. Linear trends of the contributions in 1980–2005 from source regions to surface O_3 over Japan in different seasons: spring (MAM), summer (JJA), fall (SON), and winter (DJF). Error bars are 95 % confidence intervals.
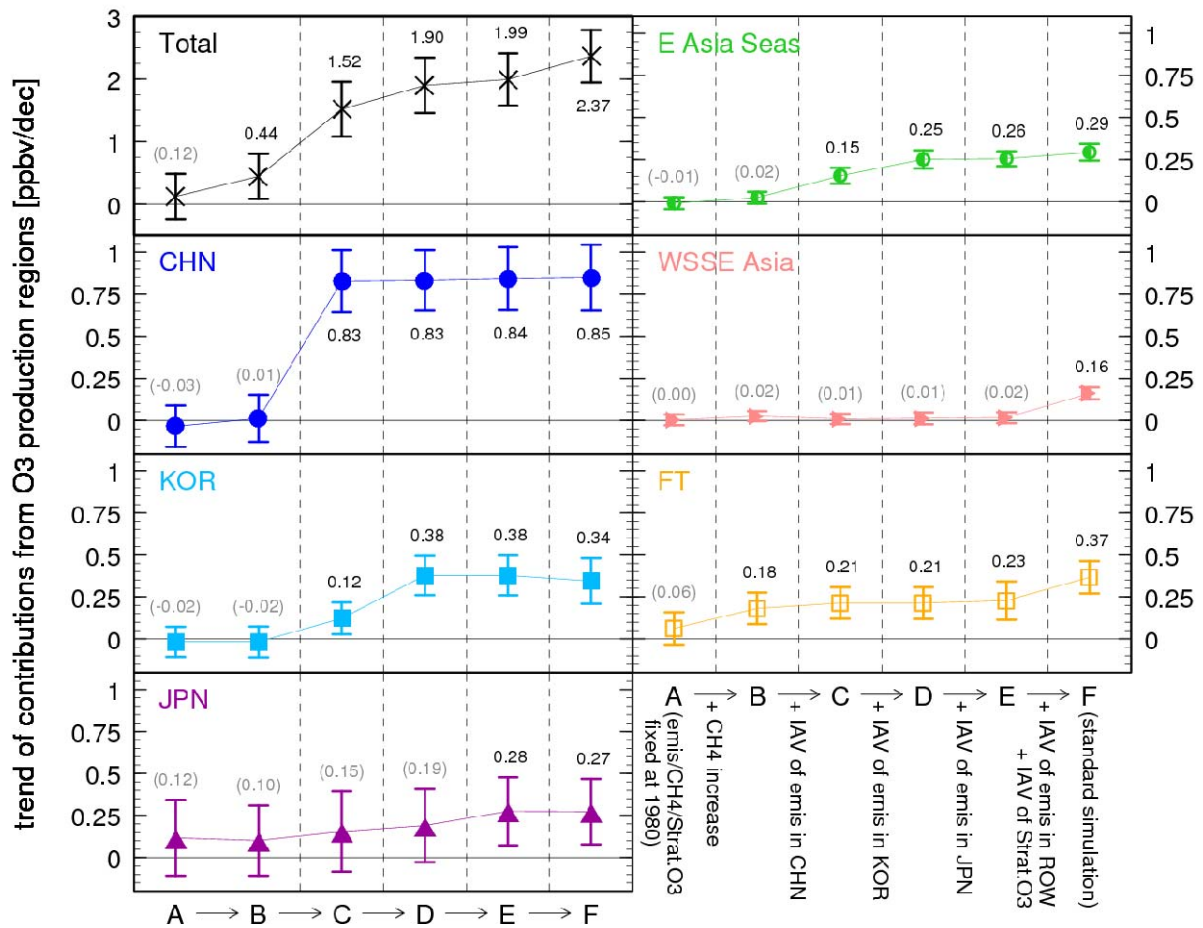
Figure 9. Linear trends of the annual mean contributions in 1980–2005 from source regions to surface O₃ over Japan in the sensitivity simulations and the standard simulation (error bars are 95 % confidence intervals). The exact values of the trends are also shown in the figure; the trends without sufficient statistical significance are shown in parentheses. The trends of each region's contribution in the simulations A–E and F (the standard simulation) are arranged from left to right in each panel.